ا مهـورية ا ـزائرية الد قراطيـة الشعبيـة

République Algérienne Démocratique et Populaire
Ministère de l'Enseignement Supérieur et de la Recherche Scientifique

UNIVERSITE DE BATNA

Faculté des Sciences de l'Ingénieur
Département d'Electrotechnique

Mémoire de Magister en Electrotechnique

Option : Machines Electriques

Présenté par Monsieur

Bouna Ould Zeidane

Ingénieur d'état en Electrotechnique de l'Université Eldjabel Gharby, Libye

Pour obtenir le diplôme de Magister de l'Université de Batna

Thème

Contribution to the Study of the Grid Connected Photovoltaic System

Case of the Domestic Load

Mémoire soutenu le / /2006
Devant le jury composé de :

Jury	Grade	Affiliation	QUALITE
BELKACEMI Mohamed	Prof.	Université de Batna	Président
AZOUI Boubaker	M.C.	Université de Batna	Rapporteur
DJARALLAH Mohamed	C.C.	Université de Batna	Co-Encadreur
MOUSSI Ammar	Prof.	Université de Biskra	Examinateur
BENOUDJIT Azeddine	M.C.	Université de Batna	Examinateur
DIB Abderrahmane	Dr.CC.	C. U. O.El-Bouaghi	Examinateur

Promotion 2003

Dedication

To all my family members,
Especially my father and mother
To all my friends…

Contents

Chapter 1
Overall background required to design a photovoltaic system

Chapter 2
Grid-connected PV system conceptions

Chapter 3
Modeling and analysis of the controlled grid-connected PV system

Chapter 4
Matlab/Simulink model Implementation and simulation results

List of symbols

Symbol	***Definition***
G	Irradiation intensity
σ	Stafan-Boltzmann constant
T	Absolute temperature
G_{ex}	Extraterrestrial irradiance
$G_{on}(n)$	Eccentricity correction factor
r_o	Annual average sun earth distance
$r(n)$	Current sun earth distance
θ_z	Solar zenith angle
E_{Ph}	Photovoltaic energy
E_g	Energy gap
h	Planck constant
c	Light speed
λ	Wavelength of light
I_{ph}	Photocurrent source
R_s	Series resistance
R_{sh}	Shunt resistance
I_{sc}	Short circuit current
V_{oc}	Open circuit voltage
P_{max}	Maximum power
V_{max}	Maximum voltage
I_{max}	Maximum current
FF	Fill factor
V_t	Thermal voltage
G_a	Ambient irradiation
m	Ideality factor
P	Active power
Q	Reactive power
L_{DC}	Inductor filter at the DC side
C_{PV}	Capacitor filter at PV output

Symbol	***Definition***
C_{link}	Linked capacitor at the inverter input
V_{link}	DC linked voltage
I_{inv}	Inverter output current
V_{inv}	Inverter output voltage
V_{PV}	PV generator output voltage
I_{PV}	PV generator output current
v_c	Output filter capacitor voltage
i_c	Output filter capacitor current
v_u	Utility voltage
i_u	Utility current
i_L	Load current
E	Irradiation energy
E_{max}	Maximum irradiation energy
t_{st}	Sunrise time
I_{sat}	Saturation current
q	Electronic charge
V_{mp}	Module voltage
I_{mp}	Module current
V_{ref}	Reference voltage
I_{ref}	Reference current
ΔT	Variation of temperature
T_{ref}	Reference temperature
α	current temperature coefficient
β	voltage temperature coefficient
N_s	Series solar cells in module
N_p	Parallel branches in module
N_{sm}	Series modules
N_{pm}	Parallel branches

Acknoledgment

I would like to use this opportunity to honestly thank Professors **************and *****for their assistance in guiding me throughout this research and for providing me with the facilities that made this work possible.

I also want to express gratitude Professor **Abd ssamed** *** the president of the searching group in ********laboratory,** for his helpful agreement that allowed me a member in this laboratory think which allowed me finish my work in this laboratory under suitable environment.

Finally, I would like to extent gratitude and thank to all my friends for their continuous helps.

General introduction

The world energy consumption has still increased due to expected rapid increase of world population, especially in the third world and in new industrialized countries because ever more humans also need ever more energy. At present, the world consumes over 8477.4 million tones oil equivalent (toe) of primary energy each year. This is roughly equivalent to $3.6x10^{20}$J. The vast majority of this energy is obtained by combustion of fossil fuels, nuclear and hydroelectricity generate approximately 7.4% and 2.7% respectively. There are problems with this present situation as the reserves of fossil fuels are limited and there is potential for global warming, [1].

Continually rapid growth is foreseen in the near future, with the world population rising from the present 6 billion to about 8 billion over the next 25 years, and is expected to grow perhaps to 10 billion people by the middle of 21^{st} century. Such a population increase will have a dramatic impact on energy demand, at least doubling it by 2050, even if the developed countries adopt more effective energy conservation policies so that their energy consumption does not increase at all over that period, [2].

Sometime in the mid-21^{st} century the world will need a new, safe, clean and economical source of energy to satisfy the needs of both developing and developed nations. The World Energy Council wrote in a published report 2000, [2]:

Renewable energies are nearly unlimited energy sources, if one compares the energy, which we receive from the Sun, with the energy demand of humankind. Moreover they are available prevailing inland or local and therefore secure. The problem is that without financial support renewable energies cannot normally compete with fossil energies. However this does not mean that it is not important to promote renewable energies according to market economic criterions in order to get even more profit from reduction in costs with mass production and from experiences with their increasing application, [3].

To cover the energy requirement, the researches are being made for conventional or renewable energy. One of the renewable energy is solar energy, which can be the main source or alternative energy source in the power generator. Excellence of using the renewable energy is clean energy and friendly to the environment. Beneficially solar radiation is equally distributed in the any place on the earth, its density isn't large, irradiation fluctuate sharply with the fickle weather, and the solar energy cannot be stored, which cause no conflict on the earth and on each one in peace. In fine details, the irradiance intensity is influenced by the factors: geographic (longitude, latitude) of the location. The location around the equator has good irradiation throughout the year, but the location around the pole particularly in winter season has little irradiation. Based on these reason, the equipment of solar energy in the tropic area is more effective than other places (subtropics and pole). The survey, the observation and measurement must be made to sure the irradiance intensity of a location. Although in the tropic area, the topography of the location and the weather also affect the irradiation. For example, the location at the mountain is often rain or cloudy. As a result, the total irradiation in one day is low, [3, 4].

Photovoltaic (PV) generation provides a good solution for distributed energy generation (DEG). PV systems provide the highest power level in the middle of the day, which coincides with the peak power requirements on the utility grid, especially during the summer. Even though PV systems are intermittent resources due to their reliance on the sun shining, the times when the energy available from the sun is at its highest corresponds to the highest demands on the utility grid. This correlation makes PV generation highly suitable as a peaking source, [4, 5].

The major problem that must be overcome when connecting PV arrays to the utility grid is to extract and export the maximum power available with a high factor quality/price. Concerning the quality of energy, the power conditioning system (PCS) that is required to convert the DC output voltage to 50 or 60Hz AC voltage at the proper level to interface to the utility at the specified distribution level, should be selected with its control system adequately. For achieving that, the work is divided into four sections.

In the first chapter, Overall background required to design a photovoltaic system is presented. This study includes solar radiation, photovoltaic generator, and power conditioning elements.

In the second chapter a general study about grid-connected photovoltaic system is given. The study concerns the system conception, types, problems encountered, technical interconnection standards requirements, etc.

The third chapter is focused on the development of different models for each components of the system followed by an analysis of some types of the controlled grid-connected PV system.

Finally, in the last chapter, the overall system is implemented in Matlab/simulink environment and the dynamic behavior of the system is analyzed; followed by a detailed interpretation.

1.1 Introduction

The photovoltaic generation is the direct conversion of solar radiation into electricity, by means of solar cells. The solar cell is a p-n junction semiconductor under illumination; it produces a direct current depended on the weather conditions.

Therefore, in this section, the study will focus on these overall backgrounds required to design a photovoltaic system, namely, solar radiation, photovoltaic generator, and power conditioning elements.

1.2 Solar radiation

In this subsection we will give an outlook study about solar radiation as the source of the photovoltaic energy.

1.2.1 Solar radiation source

The sun is a large sphere of intensely hot gases consisting, by mass, about 75% of hydrogen, 23% of helium and others (2%). Its mass and radius are respectively, 1.99 10^{30} kg and 696000 km, [6]. Hydrogen atoms fuse there to form helium and this energy is then delivered as radiation (light and heat) into space. The sun's outer surface, namely photosphere, has an effective blackbody temperature of approximately 6000 k, [2]. This mean, as view from the earth, the radiation emitted from the sun appears to be essentially equivalent to that emitted from a blackbody at 6000 k. To understand the behavior of the radiation from the sun the characteristics of the blackbody should be discussed.

The "blackbody" is an absorber and emitter of electromagnetic radiation with 100% efficiency at all wavelengths, [7]. When the temperature is known, the radiation intensity of a blackbody can be calculated using the Stafan-Boltzmann's law, [2, 6, 7]:

$$G = \sigma.T^4 \tag{1.1}$$

where: G : Irradiation intensity [W/m^2]

σ : Stafan-Boltzmann constant [5.67 10^{-8}W/m^2/k^4]

T : Absolute temperature of the body [k]

The solar irradiation intensity is measured in watts or kilowatts per square meter [W/m^2, kW/m^2]. But the radiation energy, i.e., the power integrated over a certain period of time, is given in watt-hours (also kilowatt-hours, Joules) per square meter.

1.2.2 Solar radiation outside the earth's atmosphere

Nuclear fusion reactions in the active core of the sun produce inner temperature of about 10^7 k and an inner radiation flux of uneven spectral distribution, [8]. This internal radiation is absorbed in the outer passive layers which are heated to about 6000 k and so become a source of radiation with a relatively continuous form of spectral distribution. Measurements indicate that the radiation flux, received from the sun outside the earth's atmosphere is remarkably constant. The so-called solar constant, 1367 W/m^2, defines the average amount of energy received in a unit of time on a unit of area perpendicular to the path of radiation outside the earth's atmosphere at the average distance of the earth orbit around the sun. This value fluctuates with a few percent resulted especially from the change of sun-earth distance in the orbit during a year, [2, 9].

Due to the elliptic orbit of the earth, the extraterrestrial irradiance G_{ex} on a surface normal to the sun beam on day n of the year is, [9]:

$$G_{exn} = G_{on}(n)G_o \tag{1.2}$$

with: $G_{on}(n)$ is the eccentricity correction factor. It is given by:

$$G_{on}(n) = \left(\frac{r_o}{r(n)}\right)^2 = 1 + 0.033\cos\frac{2\pi n}{365} \tag{1.3}$$

The radii r_o and $r(n)$ respectively are the annual average and the current sun earth distance at day n. The number n ranges from 1 on January 1 to 365 on December 31. The extraterrestrial spectrum is important for satellite applications of solar cells.

1.2.3 Solar radiation on the earth's surface

While passing the earth's atmosphere, the sunlight is attenuated. Some of the sunlight is absorbed by air molecules, water vapor and dust. Some is scattered, either back into space or forward to the earth surface, by ozone, water and carbon dioxide, [2, 10].

The radiation that is not reflected or scattered and reaches the surface directly in line from the solar disc is called direct or beam radiation. The scattered radiation which reaches the ground is called diffuse radiation. Some of the radiation may reach a receiver after reflection from the ground, and is called the albedo. The total consisting of these three components is called global radiation, [9, 10]. Fig. 1.1 illustrates the solar components on a tilted plane on the earth surface.

After scattering and absorption followed by partial re-radiation into space, approximately 1000 w/m^2 reaches the ground under clear weather condition. However, this amount varies greatly from one point in time to another due to atmospheric conditions and the movement of the earth with respect to the sun, [7].

The term air mass (AM), which is often used in the field of solar energy, is defined as the ratio of the path length of the radiation through the atmosphere at a given solar zenith angle, θ_z, to the path length when the sun is directly overhead . The solar zenith angle is the angle between the ground normal and the solar position vector. Fig. 1.2 shows the definition of the solar zenith angle and the air mass number.

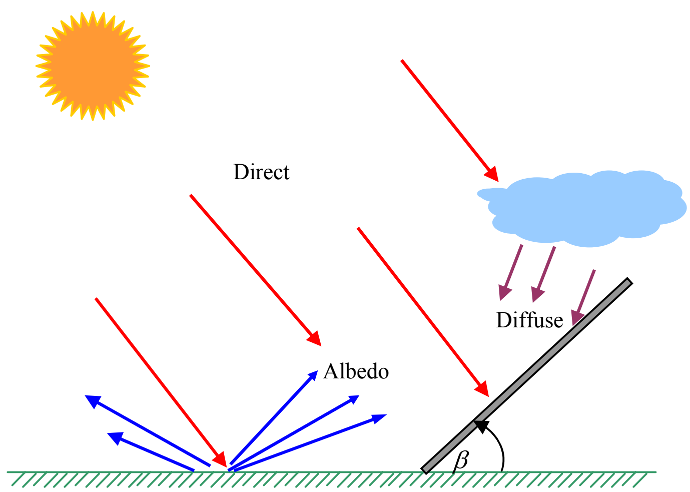

Fig. 1.1: Fractions of global radiation on the ground as received by a tilted plane, [9]

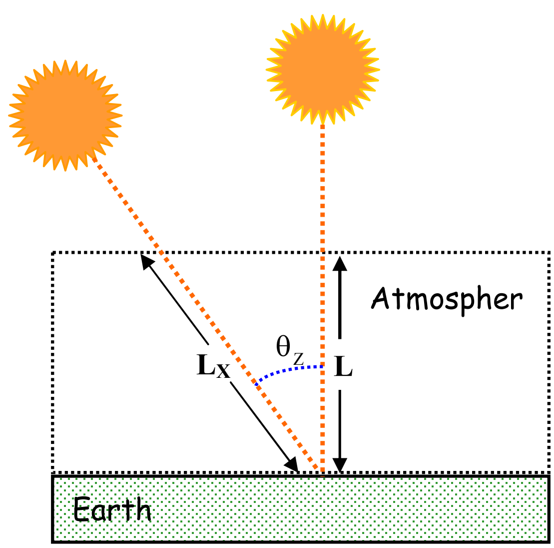

Fig. 1.2: Definitions of the zenith angle and the air mass, [7]

AM1 is defined as the air mass at the path length L_1 through the atmosphere. The air mass number for the path length L_x is $\frac{1}{\cos\theta_z}$ where θ_z the solar zenith angle. In general the air mass number is given by, [7]:

$$M = \frac{1}{\cos\theta_z} \tag{1.4}$$

When the sun is situated in the zenith above the observer, the air mass is one. Outside the atmosphere it is zero. In moderate latitudes, often $M = 1.5$ is assumed as a characteristic value, [9].

1.2.4 Algerian insolation map

Algeria is a large area country (2382000 km^2) with variety in sites leading to diversity in climate, [11]. The country receives more than 3000 hours of sunshine per year with a high level of radiation. Fig. 1.3 shows the Algeria insolation zones which can be divided into eight climate zones have approximately a homogenous insolation, [12, 13, 14]. Table 1.1 gives the received average global horizontal insolation energy.

Table 1.1: Algeria average global horizontal insolation energy

Zone	Annaba	Algier	Batna	Ouargla	In-Salah	Adrar	Tamnrasset	Janet
Zone number	1	2	3	4	5	6	7	8
Energy (kW/m^2)	4.30	4.60	5.19	5.69	6.12	6.36	6.47	6.82

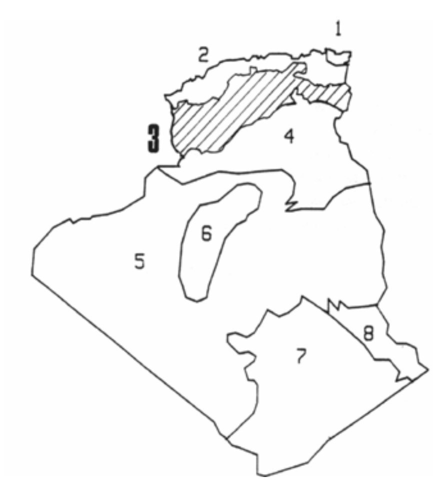

Fig. 1.3: Algeria insolation zones

1.2.5 Solar radiation measurements

In order to determine how a photovoltaic system will operate at a given geographic location, the solar radiation at the location must be measured and characterized. The solar radiation is usually measured with the help of a pyranometer or pyrhelometer.

Pyranometer as shown in Fig. 1.4, for example, is a basic instrument for measuring the global radiation. The measuring principle has based on the temperature difference between white and black painted sectors.

A precisely cut glass dome shields the sensing elements from environmental factors. By that means the measuring results is not effected by ambient temperature. When the instrument is exposed to solar radiation, temperature difference is created between the black and white sectors. This temperature difference is detected by a thermopile (a set of thermocouples) within the instrument, which then reacts by generating a small electrical signals. Finally a calibration factor converts the millivolt signal to an equivalent radiant energy flux in watts per square meter, [2].

Direct radiation can be measured by pyrheliometer. In contrast to a pyranometer, the black sensor disc is located at the base of a tube whose axis is aligned with the direction of the sunbeam. Thus, diffuse radiation is essentially blocked from the sensor surface. Furthermore, pyrheliometer, as shown in Fig. 1.5, is normally mounted on a solar tracker so that it is continually pointed directly at the sun throughout the day. However, this makes the measurements complicate and expensive.

In case of the diffuse radiation, it can be determined by subtracting the measured direct radiation from the global radiation mathematically. However, it can also be measured by applying a shadow band to the pyranometer as presented in Fig. 1.6. By this means, the sunbeam is blocked and whereby a value measured refers only to the diffuse component. By the way, the albedo radiation can be measured as well.

As shown in Fig. 1.7, for instance, the instrument consists of two identical pyradiometers. The upper measures the global radiation whereas the inner dome protects the detector from infrared radiation from the outer dome, which may change rapidly with meteorological conditions and the lower measures the reflected radiation of the ground.

Fig. 1.4: Star pyranometer, [7].

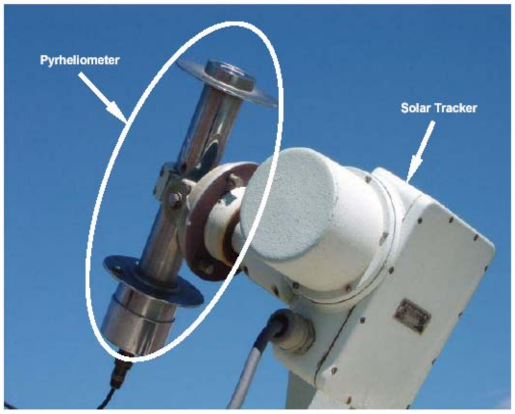

Fig. 1.5: Pyrheliometer and solar tracker, [2]

Fig. 1.6: Shadow pyranometer, [2]

Fig. 1.7: Albadometer, [2]

1.3 Photovoltaic generator

A photovoltaic generator (PVG) is the whole assembly of solar cells, connections, protective parts, supports, etc., [15]. In this section, the focus is only on cells, modules and arrays.

1.3.1 Solar cells

The direct transformation from the solar radiation energy into electrical energy is possible with the photovoltaic effect by using solar cells. And because solar cells are made of semiconductor materials (usually silicon), it is useful to give a short brief about such materials together with concentrating on solar cells it selves: its operation, structures and characteristics.

1.3.1.1 Concept of PV cells

The history of photovoltaic dates back to 1839, when the French Physicist Edmond Becquerel first observed the photovoltaic effect, [7, 16]. In 1886, American Charles Fitts constructed a selenium photovoltaic cell converted visible light into electricity with an efficiency of 1%. In the 1930s, the theory was developed for the electrical properties of silicon and other crystalline semiconductors, [7].

The silicon is one of the most semiconductor materials used to construct the PV cells. It has valence four and a diamond crystal structure. When the material is doped (Fig. 1.8), it becomes as a source of electrical energy if it is exposed to the sunlight. The photovoltaic energy conversion relies on the quantum nature of light, which carry the energy given by, [6, 8, 10, 17]:

$$E_{Ph} = \frac{hc}{\lambda} \text{ J or (eV)} \tag{1.5}$$

where: h : Planck constant;

c : light speed;

λ : wavelength of light.

The mechanism of the current generation is illustrated by the Fig. 1.9. The photons with energy in excess of the band-gap can be converted into electricity by the solar cells, and the excess of this energy is lost as heat to represent one of the fundamental losses in a solar cell.

The structure of a silicon solar cell is illustrated in Fig. 1.10, where the electrical current is extracted by front and rear contacts of the cell.

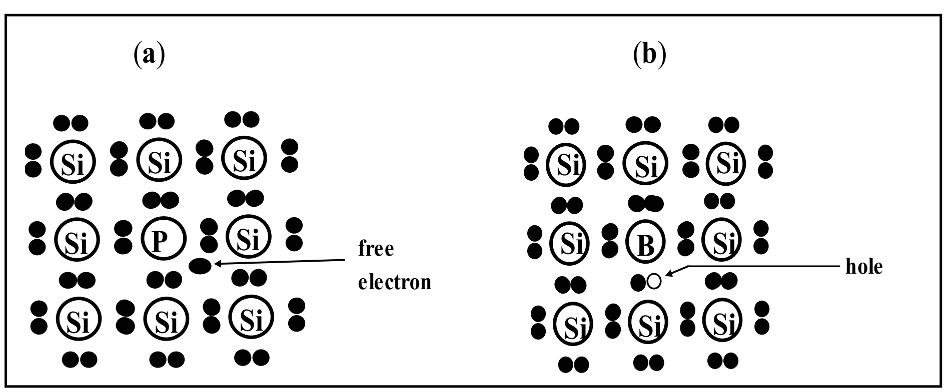

Fig. 1.8: Doping of silicon.
(a) With pentavalent atom (b) With trivalent atom, [2]

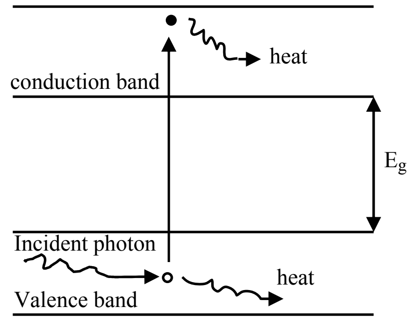

Fig. 1.9: Generation of electron-hole pairs by light, [8]

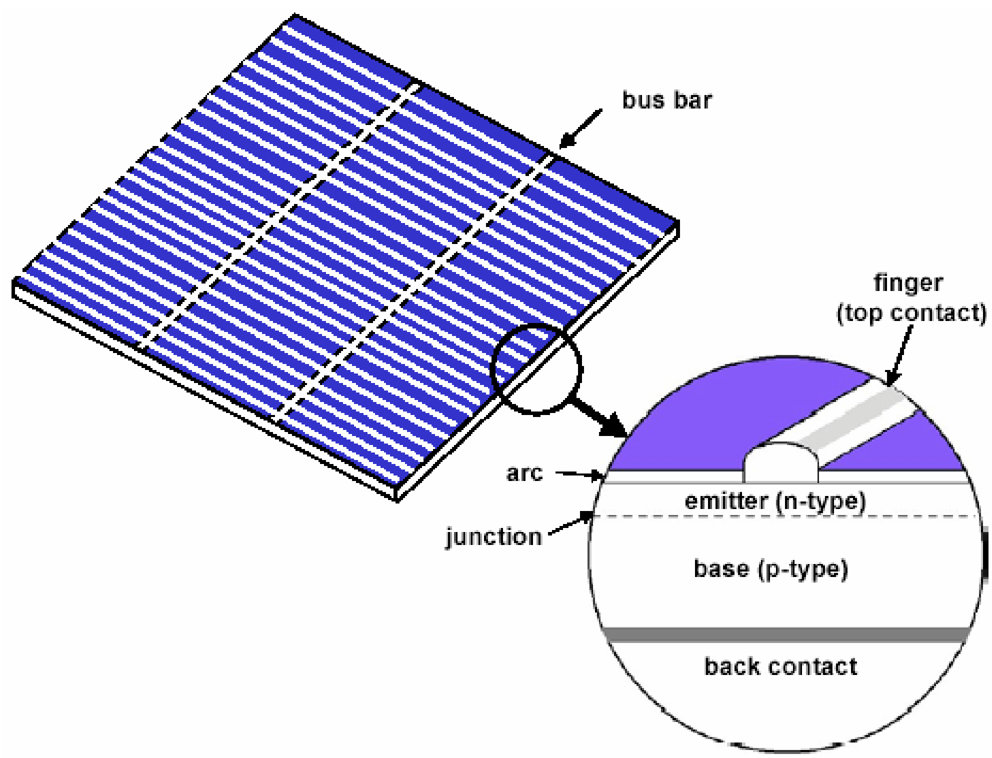

Fig. 1.10: Structure of a typical crystalline silicon solar cell, [10]

1.3.1.2 Solar cell characteristics

The typical equivalent circuit of a solar cell is given in Fig. 1.11. It is composed of a photocurrent source I_{ph}, a reverse diode D and two loss resistances (shunt resistance R_{sh} and series resistance R_s). When it is connected to an external load R_{Load}, the applied output voltage and the circulating current are V and I respectively, [2, 10, 18].

The I-V characteristic of such solar cell, when it is exposed to the sunlight and connected to R_{Load}, is given by Fig. 1.12. For a given insolation and temperature, three zones can be observed: MN region, where the current is nearly constant, PS region in which the voltage is also nearly constant and NP region which contains the maximum power point (A). So the load curve must be passing through it.

A real solar cell can be characterised by the fundamental parameters, [15] given in table 1.2.

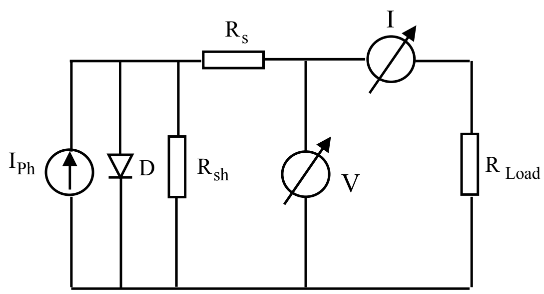

Fig. 1.11: An equivalent circuit for a PV cell or module, [2]

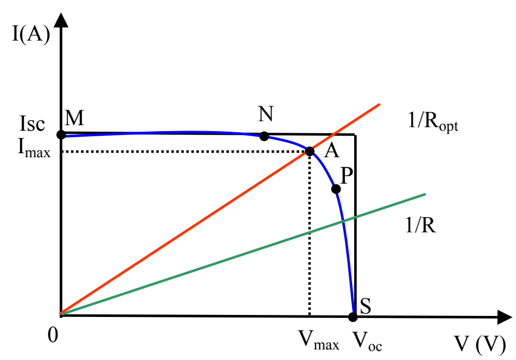

Fig. 1.12: A typical current –voltage ($I-V$) curve for a solar cell for different loads, [15]

Table 1.2: Real solar cell parameters

Parameter	Practical Equivalence	
$\mathbf{I_{ph}}$	I_{sc}	(1.6)
$\mathbf{V_{oc}}$	$\frac{mK_B T_c}{q}\ln\left(\frac{I_{Ph}}{I_o}\right) = V_t \ln\left(\frac{I_{Ph}}{I_o}\right)$	(1.7)
$\mathbf{P_{max}}$	$I_{max} V_{max}$	(1.8)
Efficiency	$\frac{P_{max}}{P_{in}} = \frac{I_{max} V_{max}}{AG_a}$	(1.9)
Fill factor (FF)	$\frac{P_{max}}{V_{oc} I_{Sc}} = \frac{V_{max} I_{max}}{V_{oc} I_{Sc}}$	(1.10)

where:

$V_t = \frac{mK_B T_c}{q}$: the thermal voltage and T_c the absolute cell temperature;

V_{max} and I_{max} : the voltage and the current at the optimum power point respecrtively;

G_a :the ambient irradiation and A the cell area. m is the ideality factor.

1.3.2 Photovoltaic module

A photovoltaic module is the connection of solar cells either in series or in parallel in order to meet specified power output requirements. Fig. 1.13 presents how the I-V curve is modified in the case when two identical cells are connected in series or in parallel.

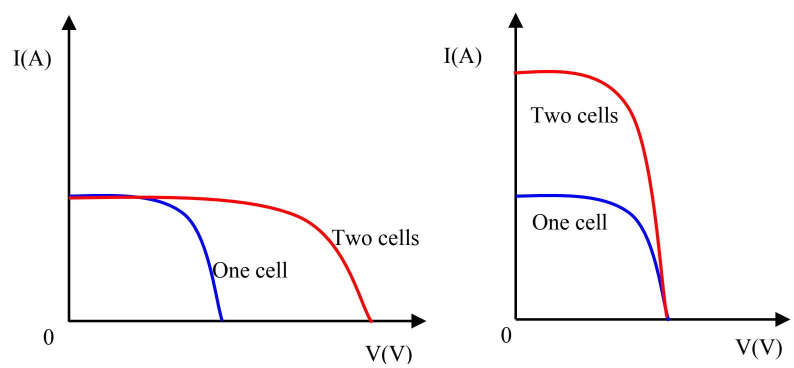

(a) (b)

Fig. 1.13: Connection of identical PV cells.

(a) In series (b) In parallel, [15]

The constructed module is an arrangement of solar cells with similar characteristics, which are encapsulated to obtain higher power values, [2]. Cells are encapsulated with various materials to protect them and their electrical connectors from the environment, [15]. The manufacturers supply PV cells in modules, consisting of N_p parallel branches, each with N_s solar cells in series, as shown in Fig. 1.14.

The overall objective of module encapsulation includes, [16]: protecting the solar cell, maximizing the amount of sunlight, user safety, etc.

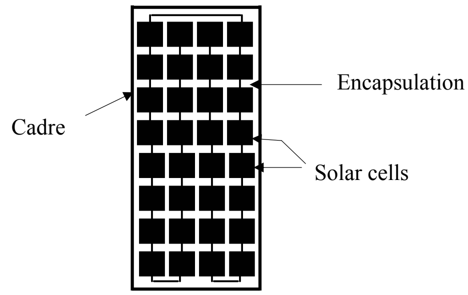

Fig. 1.14: The PV module construction

1.3.3 Module characteristics

Fig. 1.15a shows that the open circuit voltage increases logarithmically with the ambient irradiation, while the short circuit current is a linear function of the ambient irradiation. Fig. 1.15b shows that the dominant effect with increasing cell's temperature is the linear decrease of the open voltage, the cell being thus less efficient. The short circuit current slightly increases with cell temperature, [15].

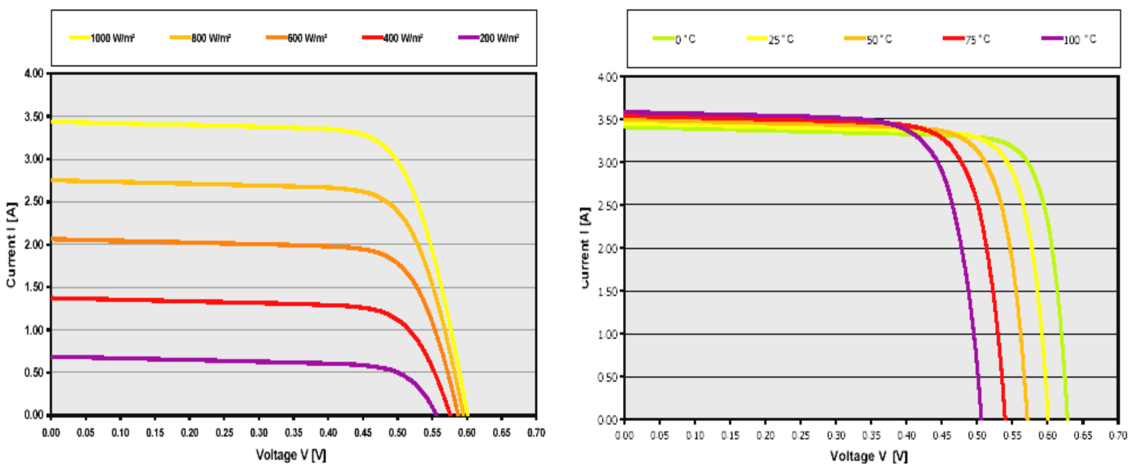

(a) (b)

Fig. 1.15: Influence of the ambient cell temperature and irradiation on the cell characteristics.
(a) The influence of cell temperature (b) The effect of the irradiation, [15]

1.3.4 Photovoltaic array

A photovoltaic array is defined as a mechanical and electrical integrated assembly of photovoltaic modules together with support structure, as required to form a direct current power supply unit.

The power output of a module is seriously affected when the module is practically shadowed or has one or more damaged cells. This problem has to be prevented for the photovoltaic array to perform efficiently. To alleviate this problem a diode is connected either for a single solar cell or for a module. In the practical, a bypass diode is connected in parallel with modules as it is shown in Fig. 1.16.

According to the inclination of tilt angles of PV arrays, there are several types in application today. Among these are, [16]: flat-Plate stationary arrays and tracking arrays.

Concerning the sizing of the PV array, three items need to be addressed: module selection, number of modules, and the orientation tilt. A several PV design packages exist in the market, [16].

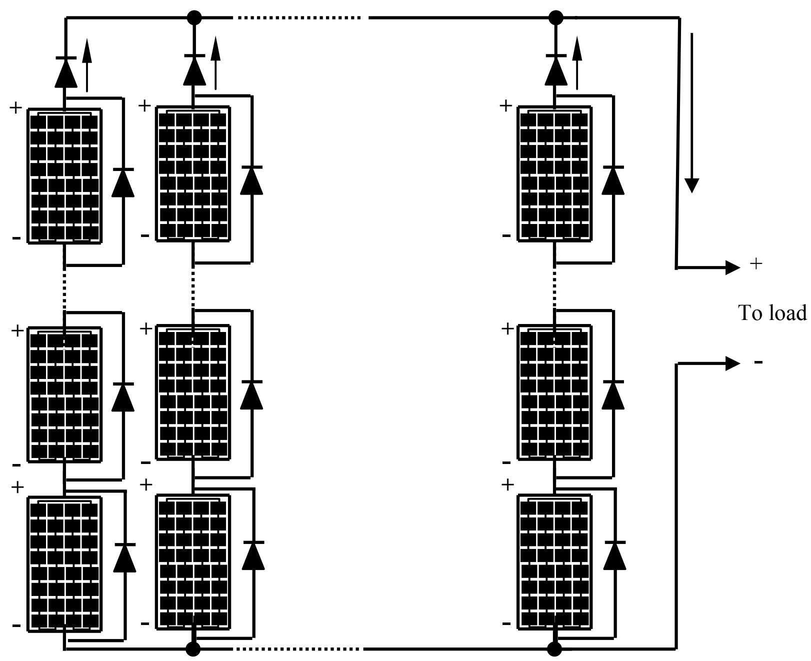

Fig. 1.16: Protection of PV array composed of series-parallel connection of modules, [16]

1.4 Power conditioning elements

According to the nature of the generated PV power (DC type) and its dependency on the weather conditions (insolation and temperature), it will become necessary to integrate the power conditioning elements: namely a DC-DC maximum power point tracking element, an inverter to convert DC power to AC type and two filters .

1.4.1 DC-DC maximum power point tracking

The purpose of the maximum power point tracking (MPPT) is to move the array operating voltage close to the MPP under changing atmospheric conditions, [19, 20]. A MPPT is, usually, a power electronic DC-DC converter inserted between the PV module and its load to achieve optimum matching, [21]. Fig. 1.17 shows an example of a buck- boost converter with its waveforms, [3, 19].

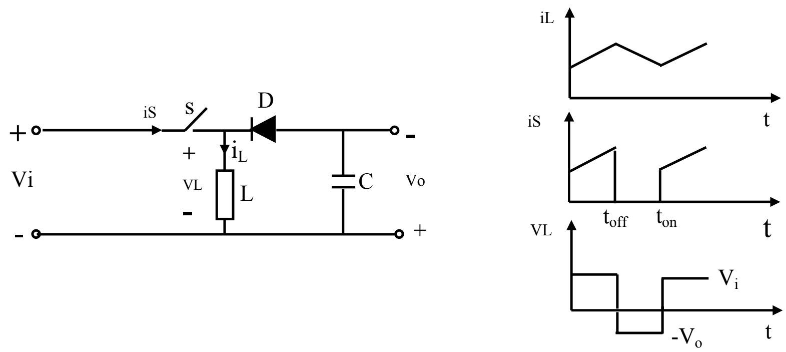

Fig. 1.17: Circuit and waveforms of DC/DC buck-boost converter

1.4.2 Inverter

According to the wave shape, there exist many types of inverters: as square-wave inverters and sine-wave inverters, etc. Since many consumers and the public grid operate on the basis of sine-wave type voltage, high quality inverters should also be able to provide this type of AC output. This voltage form can be obtained in different ways. Some of the most common layouts are pulse-width-modulation (PWM) inverters. Fig. 1.18 shows a typical configuration of single phase full-bridge inverter, [2, 4, 9, 11]. This configuration is suitable for residential applications.

It is a noticed that the filters in both sides of DC-AC converter will be treated in the next chapters.

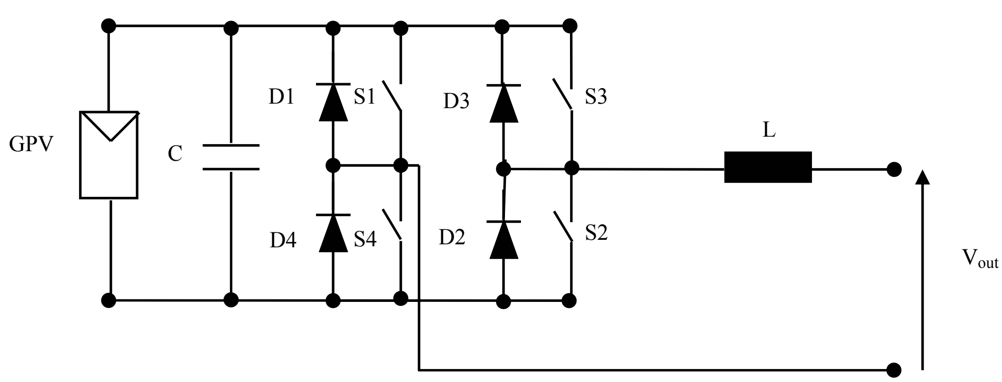

Fig. 1.18: Full bridge single phase voltage source inverter, [2]

1.5 Conclusion

The objective of this chapter was to have a complete idea about the components required for building a photovoltaic system. Therefore, the most necessary elements were studied. Solar radiation source, characteristics, and measurements were presented. PV generator (solar cells, modules, arrays) was also studied. Lastly, this study was finished by outlook for the power conditioning elements including DC-DC and DC-AC converters.

The next chapter will deal with one of the most important applications of the PV system, namely, conception of grid connected photovoltaic system.

2.1 Introduction

The conventional stand-alone systems have the advantages of simple system configuration and control scheme. However, in order to draw maximum power from PV arrays and store excess energy, battery banks are required in these systems. For high power systems, they will increase system cost and weight, and narrow the application areas. Therefore, grid-connected systems, which are designed to relieve this shortcoming, have become the primary researches in PV power supply applications, [4].

In this chapter, a general descriptive study of grid-connected PV system will be presented. This study includes: system conception, types, problems encountered, technical interconnection standards requirements, some developed programs, and finally the study will be ended by selecting studded examples of the grid-connected PV system.

2.2 Conception of grid-connected PV system

The photovoltaic power systems have made a successful transition from a stand-alone feature to large grid-connected systems. Grid-connected PV systems can vary in size, but these systems have common components. In addition to the PV components mentioned previously, the grid connected elements necessitated to be appeared here are: the power-voltage-current controller, and input/output inverter filters, as well as a metering equipment to monitor the power that is fed into the grid and vice versa, [22].

The utility grid acts as storage means for the PV arrays during daytime, therefore the load is supplied by two sources, photovoltaic source and the utility source, [17, 22, 23], as shown in Fig. 2.1 which will be proposed as a case study in this project.

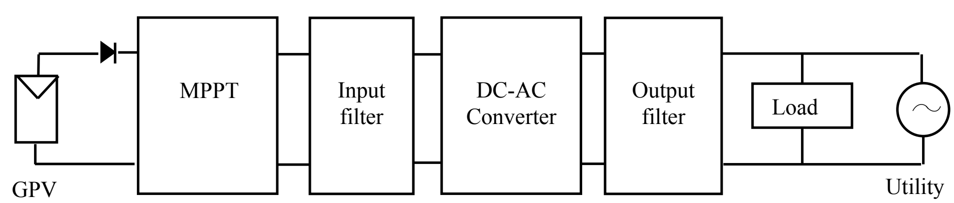

Fig. 2.1: Power circuit of a grid-connected PV system

Interconnection of power generation from PV energy sources to the grid needs static DC-DC and DC-AC converters. Connection of the converters with the distribution network is done using passive filters in order to attenuate the voltage and current harmonics, [24, 25].

Input filter

The effect of the weather conditions on the PV energy which cause fluctuations in voltage and current, make it necessary to insert the input filter to the system to adjust the DC voltage of the inverter at certain value. In the fact, there are many filters topologies as shown in Fig. 2.2a, but by taking the economical and technical considerations into account, the C filter is the suitable one. The capacitance C must be sufficient to making inverter input establishes the character of voltage source type, [24].

Output filter

Because of rapid changes in voltages and currents within a switching converter, power electronic equipment is a source of Electromagnetic Interference (EMI). Legislation and regulations require interference generated by equipment to be limited to relevant standards (ANSI/IEEE Standard 929-2000, UL-1741, and/or National Electrical Code® (NEC®). Therefore, it is also necessary to insert an inverter output filter which must be characterized by its capability to eliminate the maximum harmonics (voltage & current) exit from the inverter, [25]. Fig. 2.2b illustrates types of the output filters.

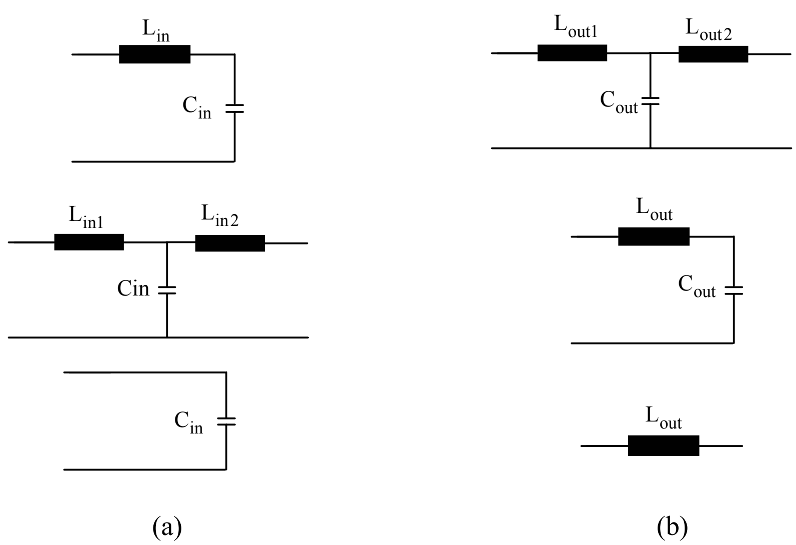

Fig. 2.2: Filtering requirements.
(a) Input filter (b) Output filter

2.3 Types of grid-connected PV systems

Two types of grid-connected PV systems are generally found: Embedded and Distributed generations, [9, 22].

The embedded PV generation, from hundreds of kW to a MW, tied to the utility distribution network can be a cost-effective solution to the problems of overload or power quality at critical points in the network. Also it is showed that it would be more cost effective to install a PV plant feeding power to a substation at the critical point rather than implementing expensive upgrades. With increasing demands of power in developing countries, embedded generation would be an attractive alternative solution for them. Currently, there are not many studies developed for distribution network of a utility in a developing country. Studies should be carried out as soon as possible to unlock a potentially large market. The PV system could provide an increased reliability in terms of supply, and could bring benefits to the economy to countries that introduces [9].

The distributed generation designated to supply consumers where the power demand is less than a few kWs (<10kW). Individual PV systems on buildings (residential or commercial) connected to the grid constitute the distributed generation. The purpose of distributed generation is to avoid buying electricity from the utility as possible. The great advantage of distributed generation from buildings is that very large area can be covered without employing additional land area.

2.4 Problems and risks involving grid-connected PV systems

The problems that should be anticipated involving interconnection of PV system to the grid would include, [26]:

- Disconnection of PV system if the grid fails (islanding problems);
- Earthing and lightning protection;
- Quality of power input to the grid;
- Effects of multiple systems on a part of the grid, particularly unbalanced single phase generation;
- Reliable metering of the power flows;
- Technical and financial risks.

Here are some details concerning these problems:

Islanding problems

The phenomenon of islanding is the operating of the PV system in the absence (poor grid reliability) of the grid. This phenomenon could cause transient over-currents when the grid power is connected back. Protection control circuits are developed and constantly revised to protect the grid and the PV from this problem and other problems such as lightning surges, short circuits and grounding, [22, 27].

Quality of power input to the grid

Many norms impose several rules to insure a high quality of power injected to the grid. For example, it states that these PV systems should be compatible with the voltage, wave shape and frequency of the grid. When either the power source/generators or the loads have solid-state equipments, harmonic currents will flow in the system. These harmonics can cause detrimental destruction to the control devices. Overrating of generators, transformers, cable, motors and circuit breakers are needed when higher harmonics are significant. Special voltage generator voltage control systems are required to avoid erratic operations, [22].

Reliable metering of the power flows

Fig. 2.2, shows the typical connection of PV system to the grid, where a reliable two-way meter is installed, so that a reliable monitoring of the power flows could be obtained. This meter should also be able to tell the consumers of any changeover of power flow. Most countries that have PV systems connected to the grid have only one-way metering, [28].

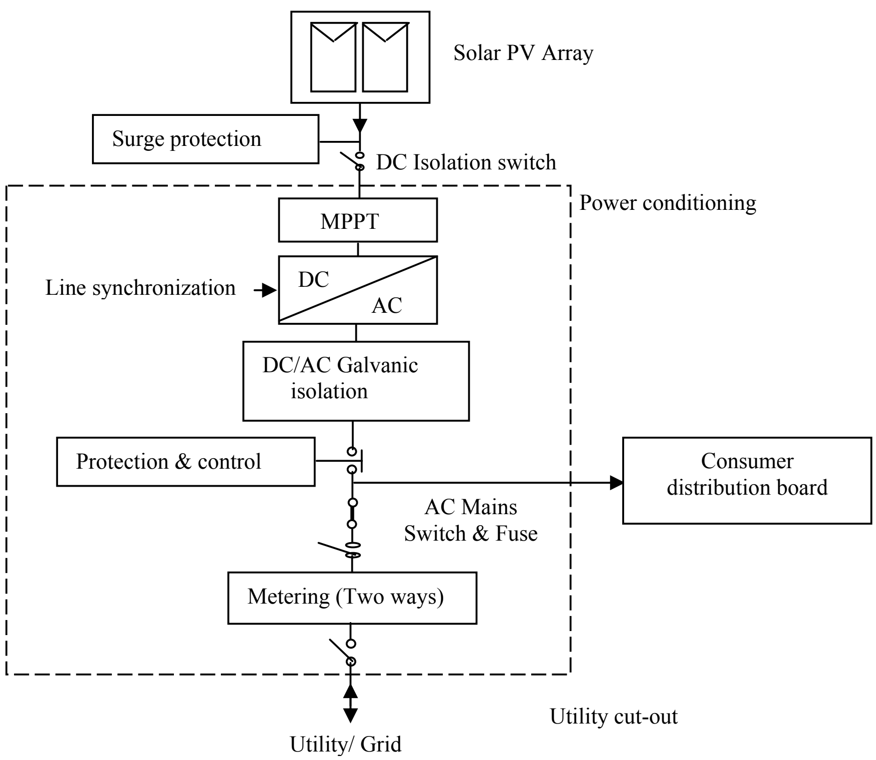

Fig. 2.3: Typical connection of PV system to the grid, [28]

Technical and financial risks

The electricity utilities present its reluctance to this technology with risks that they have no historical basis for quantifying. Some of the risks that were highlighted are, [22]:

- Technical risks: there is a possibility that the system will not be performed as specified;
- Construction risks: the possibility of going over budget, or construction of the system cannot be completed by the due date;
- Operating risks: the possibility that the system breaks down or power is unavailable when it is in demand. Other operating risks would include islanding;
- Financial limitations: high costs of finance based on the perceived risks above.

2.5 Technical interconnection requirements

The connection of the PV system with the utility grid, safety and quality for individual and companies must adhere to the standards that are developed and approved by the National standards setting authorities. The standards are as follow, [22, 26]:

- ANSI/IEEE Standard 929-2000, IEEE Recommended Practice for Utility Interface of Photovoltaic (PV) Systems.
- UL-1741, Standard for Static Inverters and Charge Controllers for Use in Photovoltaic Power Systems, Underwriters Laboratories Inc. (UL), May 1999.
- National Electrical Code® (NEC®), National Fire Protection Association, 2002.

ANS/IEEE Standard 929-2000

The IEEE 929-2000 is standard to which the PV interconnection hardware designs must adhere. This standard removes all costly and inefficient situations where different utilities require different and specialized hardware. The standard allows the PV systems to perform as expected and allow them to be installed at a reasonable cost without compromising on the safety and operational issues. IEEE 929-2000 is the first IEEE standard that allows interconnection of non-utility owned generation equipment, [26].

Their focuses are on the Power Quality (i.e. the normal operating voltage range, voltage flicker, frequency, waveform distortion and power factor), safety and protection functions (i.e. frequency disturbances and islanding protection, etc). Some of the standards are discussed briefly:

- The normal operating voltage range is selected as a protection function that responds to abnormal utility conditions. The injected current has the potential of impacting the utility voltage. As long as the PV current injection on a utility line remains less than the load on that line, the utility's voltage regulation devices will continue to operate normally.
- The voltage flicker indicated for the connection of the inverter to the utility system at the point of common coupling should not exceed the limits defined by the maximum

borderline of irritation curve identified in IEEE STD 519-1992. This requirement is necessary to minimize the adverse voltage effects to other customers on the utility system.

- The frequency of both PV and utility systems must be synchronized. The two systems should follow the frequency operating window standards in their part of their world. Utilities may require adjustable operating frequency settings for intermediate and large systems.
- The islanding protection should be included into any PV system tied to the grid. This is done by detecting the voltage and frequency of the utility grid. The IEEE 929 includes several other standards like the UL-1741. These standards are developed to assure that power that is supplied to the grid meets the harmonic content, frequency and voltage level. The main concern for the standard is to guarantee that the power conditioning unit (PCU) disconnects from the utility when the grid fails, or falls outside the operating window for voltage or frequency. Other standards that need to be followed are found in the IEEE 929 document [22].

UL-1741

The UL-1741 covers the safety aspects of the PV inverters and charges the controllers, tests for anti-islanding capabilities voltage and frequency trip points, [26]. A PV power plant feeds the generated power instantaneously into the grid by employing one or more inverters and transformers as shown in Fig. 2.4. Therefore, any PCU that passes the UL-1741 would definitely pass the criteria of the IEEE 929 standard. These PCUs do not need additional protective equipment to prevent islanding or filters to maintain power quality.

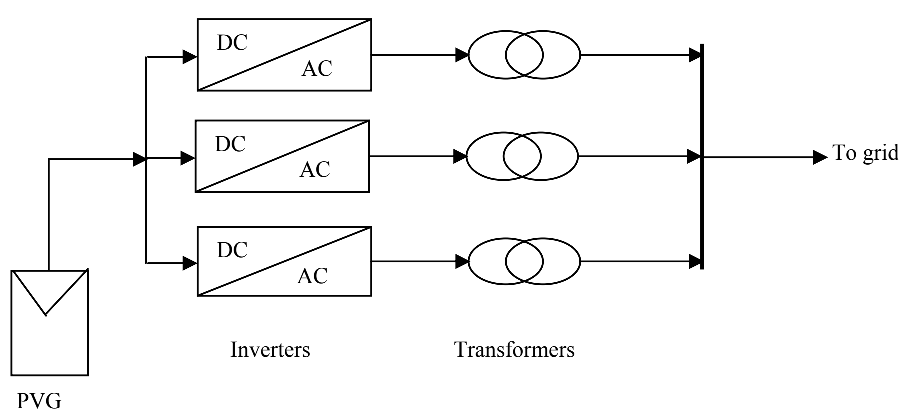

Fig. 2.4: multiple inverter PV power plant, [26]

2002 National Electrical Code® (NEC ®)

The NEC® covers the technical issues that are related to the safety and performance assuming the PV system to be customer-owned and it is connected on the load side. That will enable future PV systems to be installed using clearly defined requirements. Some of the requirements include ground fault protection, specific grounding, and over current protection, interconnection issues and others.

2.6 Benefits of grid connected PV system

In this section, the benefits of connecting a PV system to the grid will be discussed. Some of the advantages of grid-connected PV system over stand-alone systems would include the savings from wiring costs, batteries and the possibility that grid-connected PV system could sell off the surplus electricity to the utility. Some of the benefits of grid-connected PV systems are briefly discussed in the following sections, [26]:

Reduction in labor costs

By following the requirements set by IEEE, UL & the NEC®, the utility would remove the need to come out with requirements or standards of its own. The use of two-way metering also would reduce the need for separate processing of meter readings for electricity that is delivered to and from the customers.

Reduction in equipment costs

Inverters that follows the UL-1741 standards would provide safety and power quality protection, therefore eliminates the need for the utility to implement a separate protection devices on its network.

Distributed generation benefits

Studies have shown that there is a direct, measurable economic benefit of distributed generation, [26], which includes reduced energy losses in transmission and distribution lines. Other advantages would include voltage support, reactive power losses, deferred substation upgrades, deferred transmission capacity and reduced demand for spinning reserve capacity.

Environmental benefits

PV electricity generation would reduce the effects of pollution caused by conventional power generators. Looking at the green house effects, PV electricity generation would provide a better alternative to the pollution problems, [2]. Grid connected PV systems reduce the consumption of natural resources, such as coal, oil, etc, therefore diminishing the need for new power stations.

2.7 Some developed programs around the world

There are many important developed programs around the word in whole fields of renewable energy; in this section, the study focus at the developed PV Programs, especially where the grid-connected is applied.

In the United State, the Department of Energy (1970-1980) monitored household loads in one of their research programs. They evaluated and provided technical information on residential PV systems in different regions; build and monitored PV powered homes and commercial buildings, and studied their impacts on the power distribution network. This program is now superceded by the "Solar 2000" program, which aims to develop economically competitive PV systems and hence increase installed capacity in the US from 50 MW to 1000 MW by 2000 and 50,000 MW by 2010-2030, [22]. Other US Programs include the Utility PV Group (UPVG). They planned to educate utility end users as to the value of PV in their systems and introduced a cost effective and emerging PV technology in US utility grids from 1993 onwards, [22].

In Japan, Grid-connected market increases satisfactory in 2001. 50 kW for off-grid domestic application, 5960 kW for off-grid non-domestic application, and 116 000 kW for grid-connected, for grid-connected distributed applications, especially in residential sector were installed.

In year 2000 grid-connected distributed systems increased dramatically because the additional budget for Residential PV System Dissemination Program was approved to correspond to great demand for residential PV systems. Thus, the total installed capacity of grid-connected distributed systems in 2000 increase 77% from the year before, [29].

In 1992, Austria began a "200 kW Photovoltaic Rooftop Program". Financial support is provided to the householder for the building integrated, utility connected PV systems up to 3.6 kWp. The program was closely monitored to assess the feasibility of decentralized generation, [22].

In the last several years, Germany has executed important programs in the field of PV that have triggered remarkable results in market development and technology progress.

While most developing countries install stand-alone PV systems, India has planned major PV programs, including grid-connected systems up to 100 kWp. Seventy central village sized PV plants, ranging from 2 to 10 kW are now in operation. In 1993-94 further 200 kW of the same system was installed.

Installed PV capacity in Australia grew by 15% in 2000, with 3.89 MWp PV system installed. A large proportion (over 80%) of this was for installations on residential, commercial and educational buildings, a market stimulated by an Australian Government PV rebate program. The grid-connected PV market continues to grow and now represents 10% of installed capacity, [30].

2.8 Examples of grid-connected PV system

In this section, the study will be focused on the most important examples, which have been studied, to get a general idea about the different constructions, considerations, and technical methods which are used in grid-connected PV systems. For this purpose, several studies will be summarized including: Power flow control of a single distributed generation unit with nonlinear local load, [31], Optimization of photovoltaic system connected to electric power grid, [32], Utility-connected power converter for maximizing power transfer from a PV source while drawing ripple-free current, [33], Novel maximum-power-point-tracking controller for PV energy conversion system, [34].

2.8.1 Power flow control of a single distributed generation unit with nonlinear local load

This example was introduced from three phases distribution to one phase to will be suitable for our case study. It combines voltage regulation plus harmonic (current control) minimization under island mode and decoupled P and Q control under grid-connected mode with a nonlinear local load. The control does not require knowledge of the equivalent impedance of the utility grid distribution (DG) unit is connected to and yields seamless switching transients between island mode and grid-connected mode, strong P and Q regulation capability, fast enough response, and purely sinusoidal.

2.8.1.1 System description

The DG unit, as shown in Fig. 2.5, consists of a DC bus powered by any DC source or AC source with a rectifier, a voltage source inverter, an LC filter stage, an isolation transformer with secondary side filtering. The DG unit has a local load, linear or crest, and is connected to the utility grid through a TRIAC. The utility grid is modelled as an equivalent AC source with an equivalent internal impedance (Z).

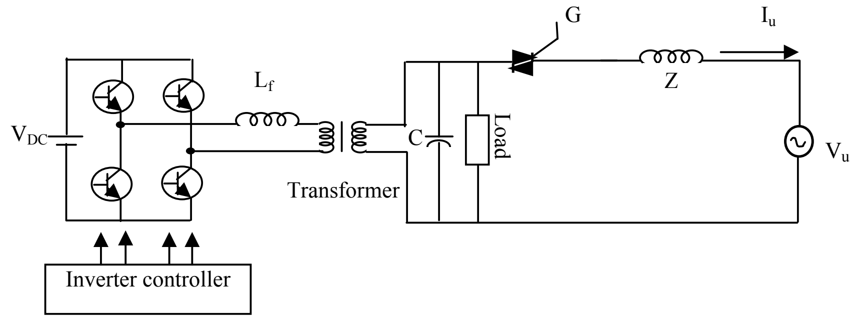

Fig. 2.5: Grid-connected DG unit with local load

2.8.1.2 Control scheme

Under island mode, the inverter conducts voltage control, where the load voltage (V_{out}) should track the given reference. The voltage control goal is strong voltage regulation, low static error in rms, fast transient response, and low total harmonic distortion (THD). If the voltage of the utility main V_u is measured and used as the reference, V_{out} will be controlled to match V_u in magnitude and synchronized in phase angle.

Under grid-connected mode, the DG unit conducts power control, where the output active power P and reactive power Q from the DG unit to the utility grid should be regulated to desired values P_{ref} and Q_{ref}. Both P_{ref} and Q_{ref} can be positive or negative, which provides possibility for the DG unit to help with the energy production and stability enhancement of the power system or sustain power supply to local load when it exceeds the capacity of the DG. The control goal of power regulation is stability, low static error, and fast response. In the switching transient from island mode to grid connected mode, even though V_{out} matches V_u before the TRIAC is turned on, transient current will still flow due to the change of the circuit topology.

2.8.2 Optimization of photovoltaic system connected to electric power grid

This example proposed the use of a PWM inverter to promote the interface of a photovoltaic system with the AC system. The main idea is to make this system to operate as a controllable voltage source connected in parallel with the power grid.

2.8.2.1 Operation principles

This work proposes the use of a PWM inverter, to promote the interface of a photovoltaic system with the ac system. The idea is to make this system to operate as a controllable voltage source connected in parallel with the power grid. By controlling the inverter output voltage phase angle and amplitude in relation to the grid voltage, it is possible to have the photovoltaic system supplying active and reactive power, independently of the sunstroke level.

2.8.2.2 Control technique and power circuit

The control technique used was developed with the objective of adjusting the inverter active and reactive power supplied to the electric grid**,** according to what can be produced by the photovoltaic system, in order to maintain the DC side inverter voltage regulated for the best possible performance. The control circuit block diagram and the power circuit for this application are presented in Fig. 2.7.

As shown in Fig. 2.7b, the control circuit is divided in two blocks: block 2 extracts the signal from the current generated by the photovoltaic modules (I_{Ph}**)** and compares it with a reference signal ($I_{Ph,ref}$), generating an error (e2). This error is multiplied by the grid voltage signal (V_u) and the result is added to this voltage (V_u)*,* originating a modified value (y2). Block1 extracts the signal from the DC-side capacitor voltage (V_c**)** and compares it with a reference signal ($V_{c,ref}$, originating an error (el). This error pass through an integral proportional circuit and it is multiplied by the grid voltage signal (V_u), which has a 90° phase shift in advance. This new signal originated (yl) is added to the modified value (y2) from block 2, resulting the PWM reference signal (V_I). Therefore, block 2 adjusts the voltage amplitude, and block 1 adjusts the load angle.

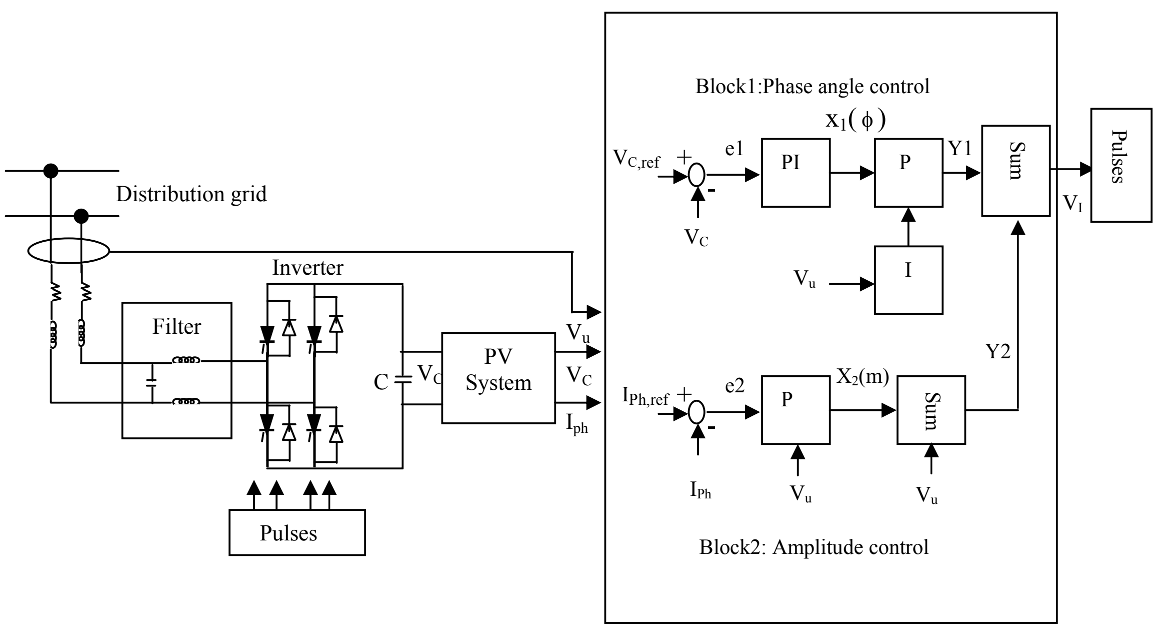

(a) (b)

Fig. 2.7: Configuration of the system.
(a) Power circuit (b) Control section

2.8.3 Utility-connected power converter for maximizing power transfer from a PV source while drawing ripple-free current

This example presents a power converter for coupling photovoltaic arrays to the utility grid. The converter draws a programmable, ripple-free of current from the photovoltaic array and injects power into the grid at unity power factor. The programmable input current feature makes this converter ideal for use with maximum power point tracking technology.

2.8.3.1 Operation principles

A power converter design for coupling solar panels to the utility grid for power generation was presented. Fig. 2.8 shows a block diagram of the system. The basic features of the system are controllable, ripple-free current drawn from the PV unit, and power injected into the grid at unity power factor. The controllable input current feature makes this design compatible with maximum power point tracking. This design has an additional unique feature in that the DC link is not kept stiff. In a conventional design, the DC link capacitor would be large enough so that AC current drawn from the link by the inverter does not create a large voltage fluctuation in the link.

2.8.3.2 Filter requirements

As seen in Fig. 2.8**,** the converter has three main filters: C_{PV}, L_{DC} and C_{link} at the output of the DC-DC converter, and L_{inv} and C_{inv} to filter out the inverter switching frequency ripple current. In a traditional design, the DC link capacitor C_{link} is designed to be large so that any ripple current drawn from the link flowing through the link capacitor causes a small voltage variation.

2.8.3.3 Control section

There are two main control sections in the system: DC-DC and DC-AC control design sections.

For controller design and simulation the DC-DC converter average model was used**.** The average model describes the converter behavior for average values of current and voltage without the switching ripple. To design the controller the DC-DC converter must be linearized. The block diagram of the system is included a DC-DC converter control scheme.

The inverter controller has two main functions. First, it must source a sinusoidal current into the grid at unity power factor. Second, it must regulate the link voltage V_{link} to a desired average value. The controller features an inner current loop and outer voltage loop. The voltage loop must be designed to regulate the average voltage of the link. When the DC link average value is lower than the desired (reference) value, the reference current decreases, which decreases the current drawn from the DC link. This causes the link voltage to increase.

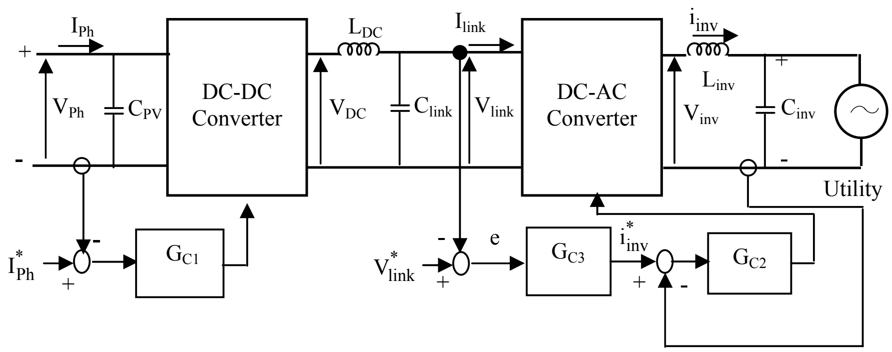

Fig. 2.8: System block diagram

2.8.4 Novel maximum-power-point-tracking controller for PV energy conversion system

In this example, the study was implemented to let the system operates at the maximum Power point to increase the output efficiency of PV arrays. The MPPT method which was used is the perturbation and observation method. Conventionally, PV energy conversion systems are composed of a DC-DC converter, a DC-AC inverter, batteries, and a center-tapped output transformer.

2.8.4.1 Proposed MPPT algorithm

The conventional MPPT algorithms use $\frac{dP}{dV} = 0$ to obtain the maximum output power point. The perturbation and observation method measures ΔP and ΔV to judge the momentary operating region, and then, according to the region, the reference voltage is increased or decreased such that the systems operates close to the maximum power point .

2.8.4.2 System configuration and control scheme

A traditional two-stage PV energy conversion system is connected between the PV array and the electrical power system. The DC-DC converter is controlled so as to track the maximum power point of the PV array and to transfer energy to the batteries and inverter. The DC-AC inverter is controlled to produce an output current in phase with the utility voltage and to obtain a unity power factor.

The system configuration of a single-stage PV energy conversion is shown in Fig. 2.9a. It is controlled so as to supply power to the load and supply surplus power with a unity power factor to the utility line. Simultaneously, system must be operated so as to track the maximum power point of the PV array. Fig. 2.9b shows the controller block diagram of the proposed single-stage system. When the system is operated in the solar generator mode, the single-stage MPPT controller is used to compute V_{ref} the according to the proposed MPPT algorithm. When the system is operated in the active power line conditioner mode, the reference voltage is a constant voltage. The voltage controller G_{vc} is used to control the voltage loop to produce the DC reference current command I_m. Then, the DC reference current is multiplied by $\sin(\omega_u t)$, which is captured from the phase-locked-loop (PLL) circuit to produce the ac reference current command i_u^*.

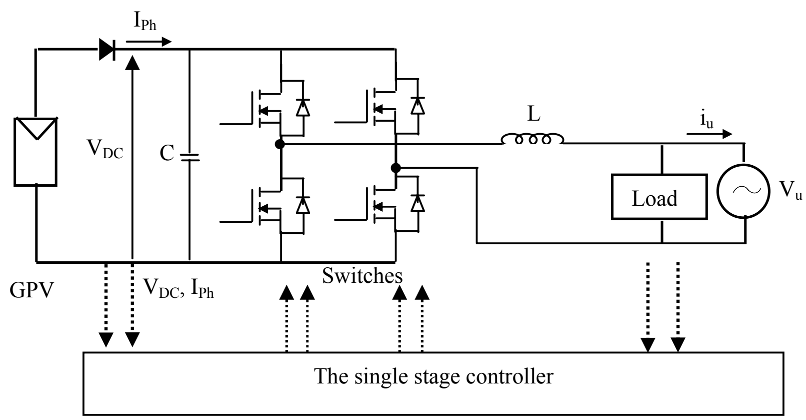

(a)

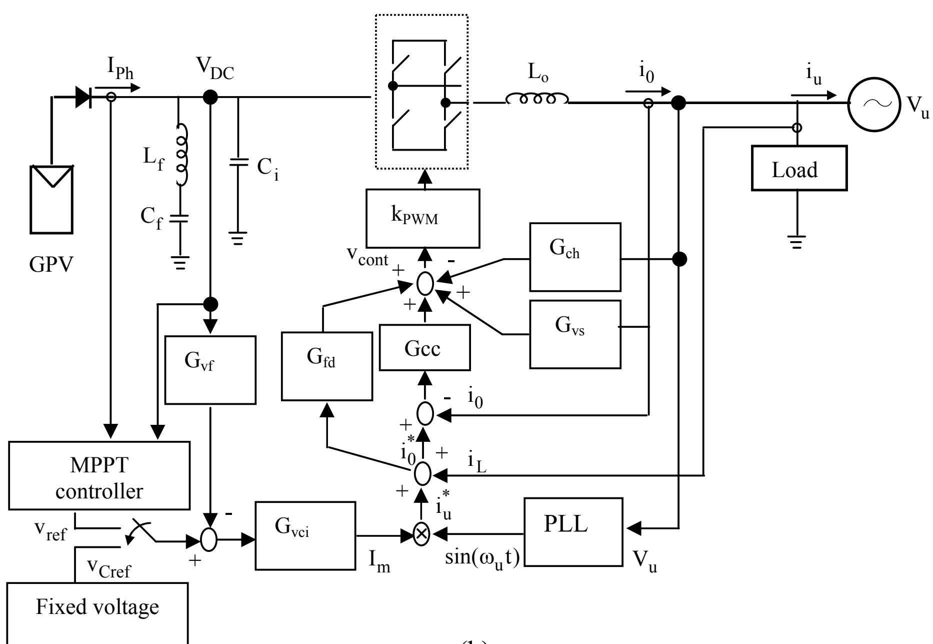

(b)

Fig. 2.9: PV energy conversion system.
(a) Power circuit (b) Controller circuit diagram

2.9 Conclusion

The purpose of this chapter was to have background information about the grid-connected PV system, as it is the case study of this work. For that, a general conception of the system is given together with: its types, problems involving the interconnection, the technical standard interconnection requirements, and the best developed programs around the word. To finish this chapter, many selected studied examples in the field are exposed. In the following chapter, modeling and analysis of the controlled grid-connected PV system will be studied.

3.1 Introduction

Any grid connected PV system can transfer powers with the grid utility, but by what and how this operation is obtained?. The operation can be reached by different controllers for different quantities (powers, voltage, and current). All this necessitates a development and analyzing of different models for different power system elements of course, including controllers models.

The main purpose of this chapter is to describe the model of each element of the proposed controlled grid-connected PV system in order to manage the system operation with maximum power and high energy quality. But first of all, let see the configurations that can be studied.

3.2 Global Configurations

In the distributed PV generation, generally many circuit configurations of topologies can be observed, [35, 36]. The general conception, without transformer, can be illustrated in the Fig. 3.1, where the inverter and its controller are detailed; meanwhile the PV generator (PVG) and the associated MPPT are given as block diagrams. As main elements shown in this figure, the following subsystems are included as well: inverter input and output filters, load, and the grid.

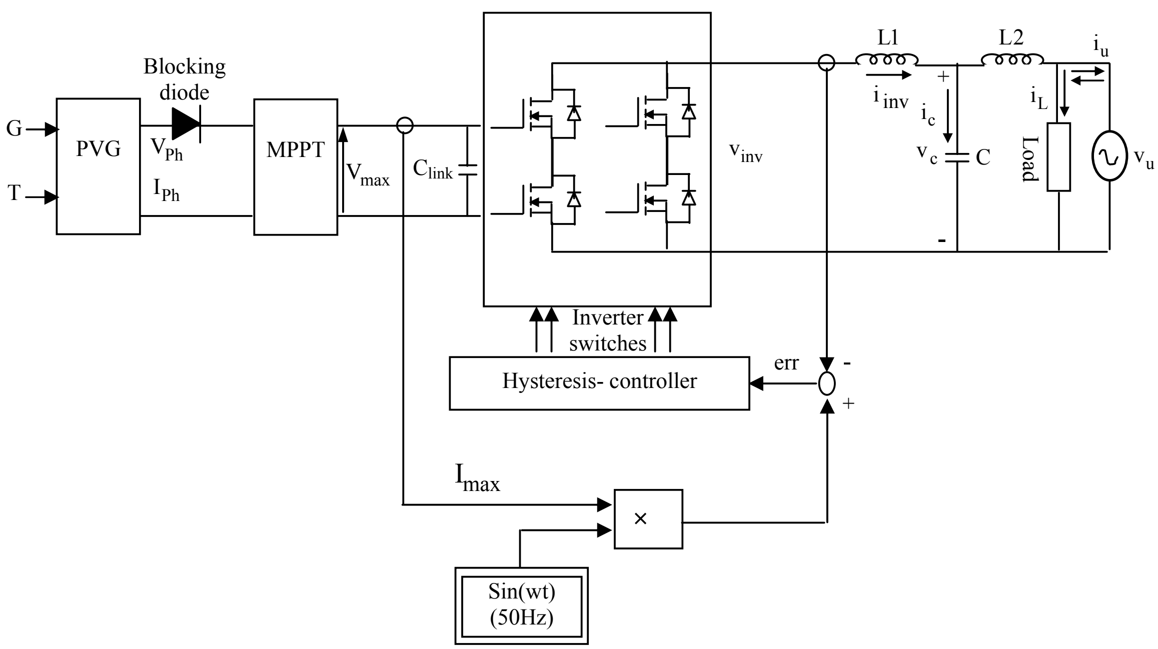

Fig. 3.1: Equivalent circuit of the proposed PV controlled grid-connected system

3.3 System modeling

The power system elements and the related parameters need to be modeled are: solar irradiation, PV generator, MPPT, inverter and its control system, load, and utility models.

3.3.1 PV array model

As it is known, the PV array performance depends totally on the climatic conditions essentially temperature and insolation. Thus, the model for the insolation versus time, t in hours, can be given as follow, [12, 37]:

$$E = E_{max} \sin(\pi \frac{t - t_{st}}{12}) \qquad (3.1)$$

where: E_{max} : the maximal insolation (W/m^2);

t_{st} : sunrise time (hours).

As example, Batna site is taken for calculation of the daily insolation, where the maximal insolation in period of summer is 1000 W/m^2 and the sunrise is 6h^{00}.

Meanwhile, the PV array model can be obtained as accumulation of its basic component (solar cell). The solar cell equivalent electrical circuit, when neglecting the internal shunt resistance, can be represented by a one-diode model as shown in Fig. 3.2, [2, 7, 11, 18, 19, 38, 39, 40, 41, 42]. This model is considered as the general familiar model.

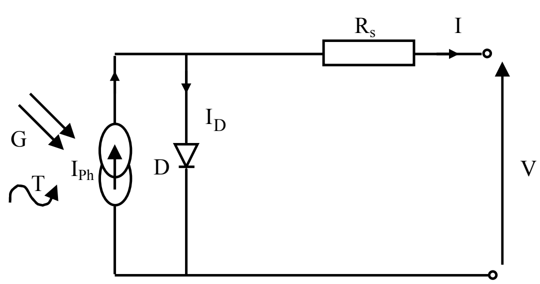

Fig. 3.2: An equivalent circuit of a solar cell

The I-V characteristics of a solar cell is given by the following equation; where the net current is the difference between the photocurrent and the normal diode current as follow:

$$I = I_{Ph} - I_D = I_{Ph} - I_{sat}\left\{\exp\left[\frac{q}{mK_B T}(V + R_s I) - 1\right]\right\} \qquad (3.2)$$

where: I_{Ph} : Photocurrent in Ampers;

I_{sat} : Saturation current in Ampers;

q : Electronic charge in Coulombs;

K_B : Boltzman constant in Joules per Kelvin.

T : Junction temperature in Kelvin;

m : Ideality factor.

In this model, the saturation and photocurrent are varied with temperature and insolation according to the following equations, [38, 43]:

$$I_{sat} = I_{or}\left[\frac{T}{T_{ref}}\right]^3 \exp\left[\frac{qE_g}{K_B T}\left(\frac{1}{T_{ref}} - \frac{1}{T}\right)\right] \tag{3.3}$$

$$I_{Ph} = \left[I_{SC} + K_I (T_C - 25)\right]\frac{G}{100} \tag{3.4}$$

where: I_{or} : the saturation current at T_{ref} (the reference temperature in K);
E_g : band gap of the semiconductor used;
G : insolation in W/m^2.

In a general, there are many models to represent the PV generator I-V characteristics. In this work, the following model is chosen according its simplicity to carryout, [11, 37]:

$$I_{ref} = I_{sc}\left\{1 - C_1\left[\exp\left(\frac{V_{ref}}{C_2 V_{oc}}\right) - 1\right]\right\} \tag{3.5}$$

where:

$$C_1 = \left(1 - \frac{I_{mp}}{I_{sc}}\right)\exp\left(\frac{-V_{mp}}{C_2 V_{oc}}\right) \tag{3.6}$$

$$C_2 = \frac{\left(\frac{V_{mp}}{V_{oc}} - 1\right)}{\ln\left(1 - \frac{I_{mp}}{I_{sc}}\right)} \tag{3.7}$$

This model requires three measured points in order to define this curve, namely the open circuit voltage, the short circuit currant and the maximum power point.

Adaptation of equation (3.5) to other levels of insolations and temperatures are carried out using the following equations, [43]. These equations shift any point (V_{ref}, I_{ref}) of the reference $I - V$ curve to a new point (I, V).

$$\Delta T = T - T_{ref} \tag{3.8}$$

$$\Delta I = \alpha\left(\frac{G}{G_{ref}}\right)\Delta T + \left(\frac{G}{G_{ref}} - 1\right)I_{sc} \qquad (3.9)$$

$$\Delta V = -\beta\Delta T - R_s\Delta I \qquad (3.10)$$

$$V_{new} = V_{ref} + \Delta V \qquad (3.11)$$

$$I_{new} = I_{ref} + \Delta I \qquad (3.12)$$

where α and β are the current and voltage temperature coefficients respectively.

For a generator photovoltaic consists of N_{sm} series and N_{pm} parallel modules:

$$V_{PV} = N_{sm}V \qquad (3.13)$$

$$I_{PV} = N_{pm}I \qquad (3.14)$$

3.3.2 Maximum power point tracker (MPPT) model

The dependence of power generated by a PV array and its maximum power point (MPP) on atmospheric conditions, make it necessary to insert a technical method in the system so that the maximum available power is being supplied to the grid. Many methods for tracking MPP had been proposed.

Two different control variables are often chosen to achieve the maximum power control, [19, 21]:

Voltage-Feedback Control

The solar array terminal voltage is used as the control variable for the system. The system keeps the array operating close to its maximum power point by regulating the array's voltage and matches the voltage of the array to a desired voltage. However, this has the following drawbacks:

- The effects of the insolation and temperature of the solar array are neglected;
- It cannot be widely applied to battery energy storage systems.

Therefore, this control is only suitable for use under constant insolation conditions, such as a satellite system, because it cannot automatically track the maximum power point of the array when variations in insolation and temperature occur.

Power-Feedback Control

Maximum power control is achieved by forcing the derivative (dP/dV) to be equal to zero under power feedback control. A general approach to power feedback control is to measure and maximize the power at the load terminal. This has an advantage of unnecessarily knowing the solar array characteristics. However, this method maximizes power to the load not power from the solar array. Although a converter with MPPT offers high efficiency over a wide range of operating points, but for a bad converter, the full power may not be delivered to the load due to power loss. Therefore, the design of a high performance converter is a very important issue.

From many algorithms which can be obtained, two algorithms often used to achieve the MPPT: the perturbation and observation (P&O) method and the incremental conductance (IC) method, [19, 21].

The perturbation and observation method has been widely used because of its simple feedback structure and fewer measured parameters. The peak power tracker operates by periodically incrementing or decrementing the solar array voltage. If a given perturbation leads to an increase (decrease) in array power, the subsequent perturbation is made in the same (opposite) direction. In this manner, the peak power tracker continuously hunts or seeks the peak power conditions.

The solar array terminal voltage can be adjusted relative to the MPP voltage by measuring the incremental and instantaneous array conductance ($\frac{dI}{dV}$ and $\frac{I}{V}$, respectively). The control flowcharts of these methods are shown in Fig. 3.3.

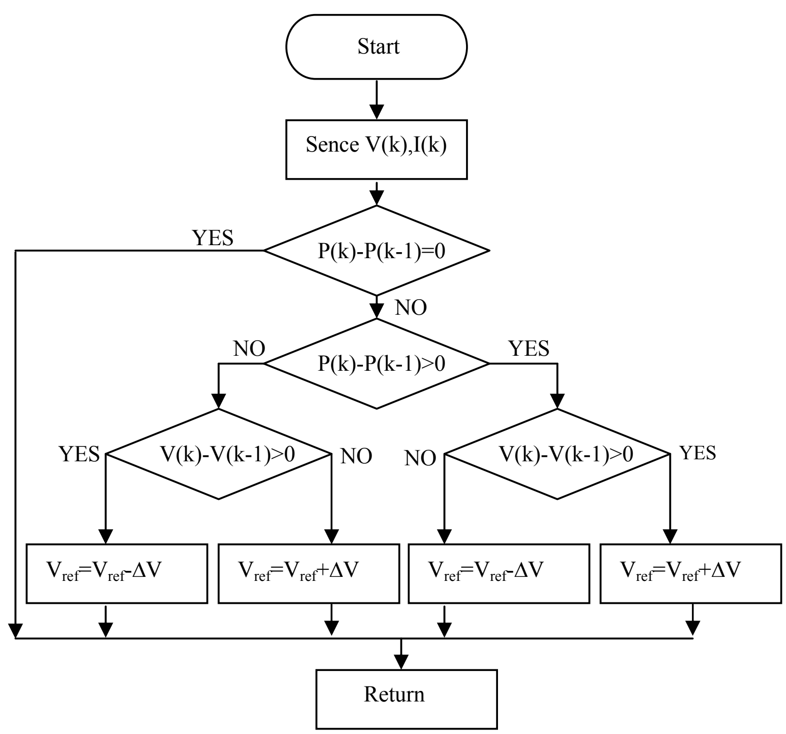

(a)

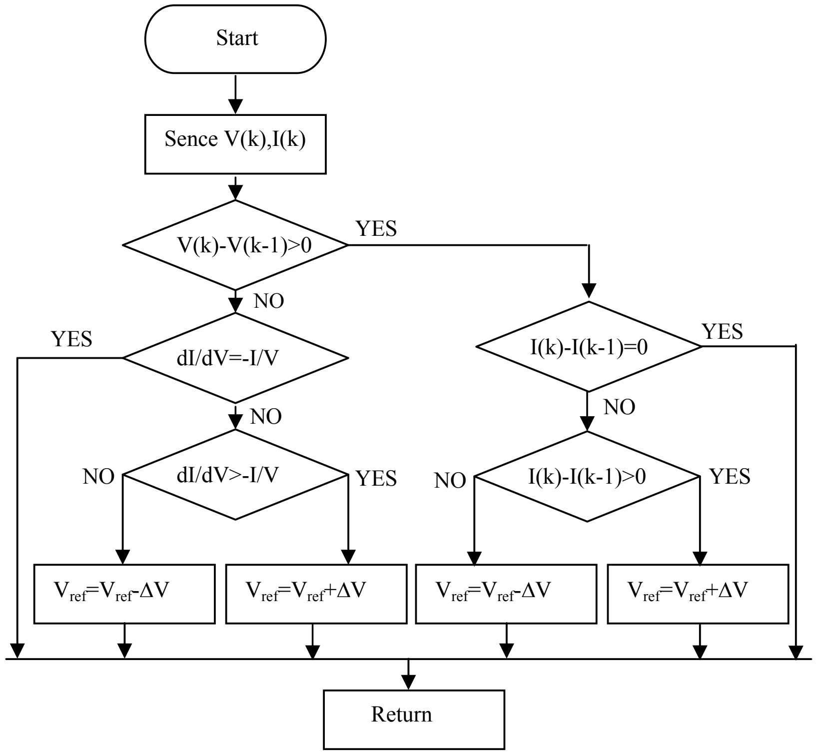

(b)

Fig. 3.3: Control flow chart.
(a) Perturbation and observation method (b) Incremental conductance method, [19]

3.3.3 Inverter controllers

The inverters are widely used in power applications where a 0-400 Hz sinusoidal signal is required, namely as an Uninterruptible Power Supply (UPS) or as a motor drive. They are also widely used in photovoltaic systems as a Remote Area Power Supply (RAPS) or as a grid connected power generator, [44, 45]. In the case of grid-connected PV system, different inverter topologies and controllers are usually used.

3.3.3.1 Inverter topology

Most inverters generate in one way or another pulse width modulated (PWM) signal, which is filtered to finally produce a low-distortion sinusoidal signals (voltage and current). The general types of PWM inverter are: Sinusoidal PWM, Harmonic elimination principle, Hysteresis (Adaptive current control PWM), and Phase-shift PWM, [46, 47, 48, 49, 50].

In addition to the inverter waveforms generation principals mentioned in chapter 1, there are many structures on which the grid connected PV inverters must be build. A three topologies can be identified in such applications, namely: central inverter, string inverter and integrated inverter, [35, 36].

Moreover, because the desired power level plays a significant role in switching type selection, therefore for grid-connected PV domestic load systems, MOSFET switches are usually chosen, where they are suitable for low power, high frequency applications. They range of tens Amperes and hundreds of Voltages, [46, 47, 48].

3.3.3.2 Controlled grid connected PV system: an overview

Most grid-connected PV systems use voltage-source inverters (VSI) type in the DC-AC conversions interfaces. These interfaces utilise various control strategies and circuit configurations to transfer powers and to shape the utility line current, making it follow a reference sinusoidal waveform. Some of the widely used control strategies are: power-current controlled, power controlled, and current controlled grid connected PV systems, etc.

3.3.3.2.1 Power-current controller

This type of system combines current control (harmonic minimization), associated with voltage regulation, under island mode, and decoupled P and Q control for grid-connected mode with a nonlinear local load, [31].

a) Voltage and Current Control

For high quality of V_{out} with strong regulation, low total harmonic distribution (THD), and overload protection, a dual-loop voltage and current control structure is used as shown in Fig. 3.4a, where the inner loop is for current control and outer loop is for voltage control. A robust servomechanism controller (RSC) is used for voltage control and a discrete-time sliding mode controller (DSMC) is used for current control, the details of this approach have been given in, [51]. The DSMC is used in the current loop to limit the inverter current under overload condition because of the fast and no overshoot response it provides. The RSC is adopted for voltage control due to its capability to perform zero steady state tracking error under unknown load and eliminate harmonics of any specified frequencies with guaranteed system stability. The theory behind the RSC is based on the solution of robust servomechanism problem (RSP), [52].

b) Active and Reactive Power Control

Since the DG unit uses a voltage source inverter with a strong voltage control, its output active and reactive power are determined by the unit's output voltage, including magnitude and phase angle. Since the DG unit output voltage control already exists, the task of the power controller is to generate voltage command for the voltage controller based on the desired power values P_{ref} and Q_{ref} and actual values P and Q as illustrated in Fig. 3.4b.

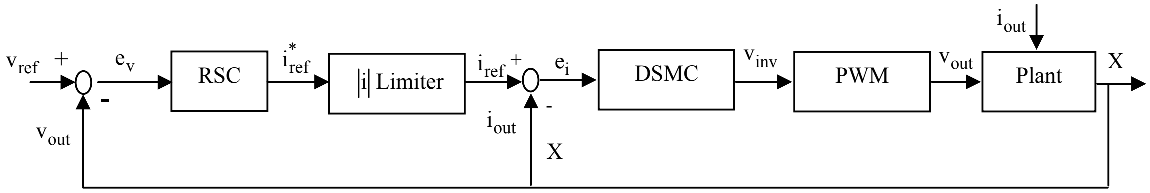

(a)

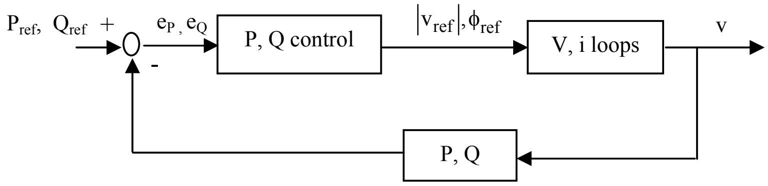

(b)

Fig. 3.4: Power-current control structure.
(a) Current control (b) Powers control

3.3.3.2.2 Power controller

Remembering that, the equivalent circuit of the grid, as a load on PV, is shown in the Fig. 3.5, where the utility voltage (V_u) is a pure sinusoidal and it is taken as reference.

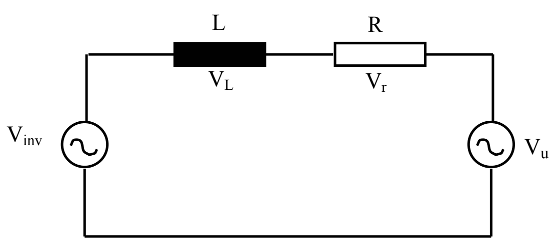

Fig. 3.5: Equivalent circuit of the load- grid

With the variation of the solar incidence, the photovoltaic system power will change. Therefore, this control should act on the inverter active power supply to keep the DC voltage on the DC side unchanged and to increase the degree of system stability. In this sense, a closed loop voltage control must be used to act on the load angle variation, and, consequently, on the DC-AC power adjustment. The control also modifies the inverter amplitude voltage, using the DC link capacitor, to supply reactive power to the grid when there is little or no solar insolation. In this way, it will function as a generator and /or as a capacitor, according to the system need, [32, 53, 54].

The active and reactive power flows in the system are not uncoupled. In fact, the active power (P) depends predominantly on the phase angle or load angle (δ) between the inverter (V_{inv}) and system voltages (V_u), and the reactive power (Q) is a function of the magnitudes of these voltages, as shown in Fig. 3.6 and equations (3.15) and (3.16), where L_C is the coupling inductance and f is the system frequency. According that, the power flow adjustment of the inverter unit, connected in parallel with the main grid, can be performed by controlling the inverter voltage magnitude and angle (V_{inv} and δ).

$$P = \frac{V_{inv} V_u}{2\pi f L_C} \sin\delta = P_{max} \sin\delta \tag{3.15}$$

$$Q = \frac{V_{inv}^2}{2\pi f L_C} - \frac{V_{inv} V_u}{2\pi f L_C} \cos\delta \tag{3.16}$$

From equations (3.15) and (3.16) the inverter output voltage magnitude and the angle δ can be expressed as follow:

$$\delta = \tan^{-1}\left(\frac{P}{\frac{V_{inv}^2}{2\pi f L_c} - Q} \right) \tag{3.17}$$

Or

$$V_{inv} = \sqrt{2\pi f L_c \frac{P + Q\tan\delta}{\tan\delta}} \tag{3.18}$$

The control can be justified, for example, by using proportional integrator (PI) as:

$$\delta = k_P(\delta_{ref} - \delta) + k_I \int (\delta_{ref} - \delta) d\delta \tag{3.19}$$

$$V_{inv} = k_P(V_{inv_{ref}} - V_{inv}) + k_I \int (V_{inv_{ref}} - V_{inv}) dV_{inv} \tag{3.20}$$

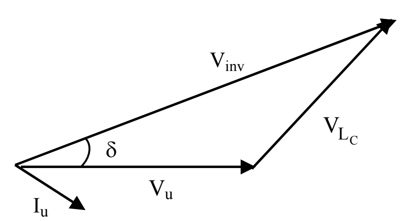

Fig. 3.6: Voltage phasor diagram

3.3.3.2.3 Current controllers

There are two broad categories of inverter current controllers: classical current controller laws (P, PI or PID), and hysteresis band controller.

a) Classical current controller

In this type, the controller uses both current and voltage control, but the voltage control loop is usually weakly integrated and its main purpose is to increase the stability and response of the system. Therefore, in addition to using the inverter output current, the capacitor voltage is also sensed and fed back to the control circuit in an outer feedback control loop such that it is constrained to follow a reference sinusoidal waveform. This will ensure both sinusoidal capacitor voltage and inverter output current, and consequently a sinusoidal utility line current, [33, 45, 55,]. Fig. 3.7 shows the resulting control scheme.

***Principle of* Operation**

The actual capacitor voltage, $v_c(t)$, is compared with its reference voltage waveform, $v_c^*(t)$, and the difference is passed through a proportional controller (k_{PV}). The output of the controller, $e_v(t)$, is then summed with the difference between the actual inverter output current, i_{inv}, and its reference waveform, i_{inv}^*, to produce the error signal $e_c(t)$. The latter signal is passed through a proportional controller in the current control loop, and the output is compared with a fixed switching frequency triangular waveform in a hard limiter. The output of the hard limiter controls the inverter switching devices such that the error between the actual capacitor current and voltage and their respective reference waveform is reduced.

Referring to Fig. 3.7, the inverter output current, capacitor voltage, and hence the utility line current, are determined by the value of the error signal e (t), which is obtained through a combination of $v_c(t)$, $i_{inv}(t)$, $e_v(t)$, $e_c(t)$ and the inverter output current and capacitor voltage command signals, $i_{inv}^*(t)$ and $v_c^*(t)$ respectively, as:

$$e(t) = k_{pc}(k_{pv}(v_c^*(t) - v_c(t)) + i_{inv}^*(t) - i_{inv}(t)) \tag{3.21}$$

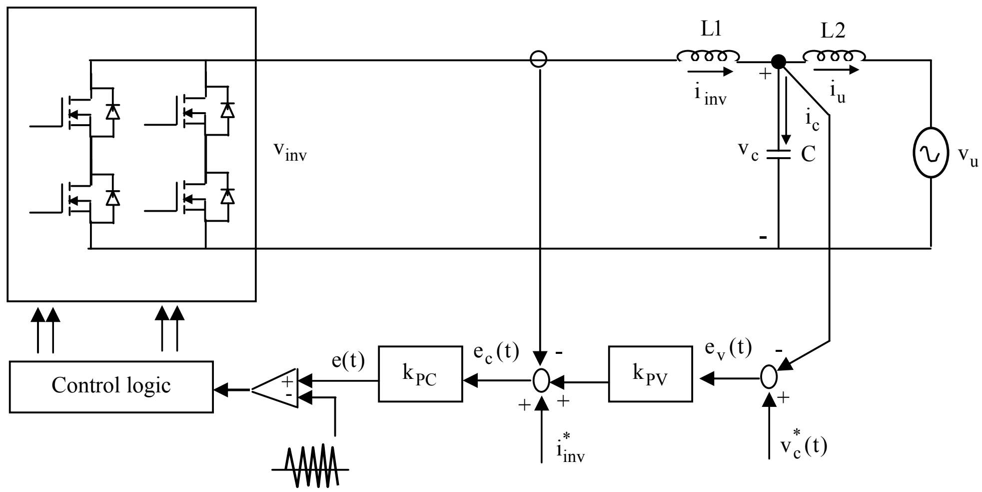

Fig. 3.7: Inverter and its control scheme

b) Hysteresis band current controller

Basically, a current controller is usually preferred to follow the current command in some apparatus (harmonics minimization). Various techniques for current controller have been proposed in recent years. Among these techniques, the hysteresis current controller is a rather popular one, [40].

The discussion on the harmonics of the PWM output voltage wave has been based on the assumption that the DC link voltage is ideally filtered. The condition is far from true, where a considerable amount of ripple may be present. The adaptive or hysteresis band current control PWM technique explained here may be adopted to overcome this problem. The technique is based on current control as explained in Fig. 3.8a, in contrast to voltage control. The control circuit generates the sine reference current wave of desired magnitude and frequency, which is compared with the actual phase current as shown in Fig. 3.8b. As the current exceeds a prescribed hysteresis band, the upper switch in the half-bridge is turned off and the lower is turned on. As a result, the output voltage is transitioned from V_{DC} to $-V_{DC}$ and current starts to decay. As the current crosses the lower band limit, the upper switch is turned on and the lower is turned off. To limit the maximum switching frequency (MSF), lockout circuits are usually incorporated, [48].

The actual current wave is thus forced to track the sine reference wave within the desired hysteresis band by back-and-forth switching of upper and lower switches. The inverter then essentially becomes a current source type instead of a voltage source type, and peak-to- peak current ripple is controlled adaptively within the hysteresis band irrespective of

V_{DC} fluctuation. The rms ripple current, which is indirectly related to peak-to-peak ripple current, is thus closely controlled, minimizing heating losses, [46].

The hysteresis current controller is considered a rather popular current controllers, for its easy implementation, quick response, maximum current limit and insensitive to load parameter variations, [39, 48]. Moreover, the dynamic current tracking of the inverter output to its target value in minimal time, while yielding feedback switching, can be achieved easily using this type of controller, [56]. Therefore, it will be chosen to control the inverter in our proposed system.

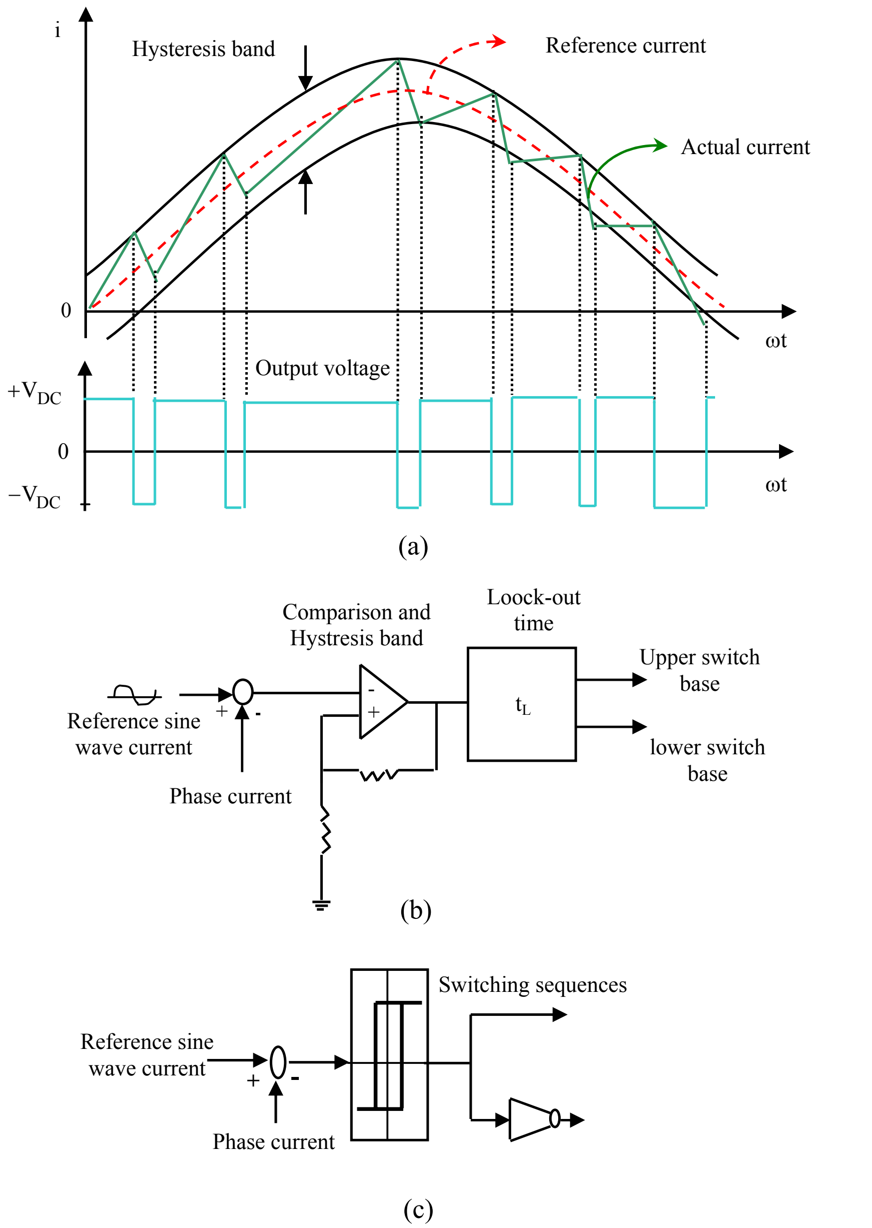

Fig. 3.8: Hysteresis technique control.
(a) Principle of hysteresis bands (b) Hysteresis block diagram,
(c) Switches sequences, [46]

3.3.4 Output filter model

Connection of the converters with the distribution network is done using passive filters in order to attenuate the voltage harmonics caused by the pulse width modulation (PWM) to levels in compliance with related standards. In addition, improvement of reactive power export to the connected grid is constrained by the filter design, [55].

By adding an inductor to the LC-filter, an LCL-filter is obtained. The line-side inductors of the LCL-filter prevent current harmonics injected by parallel loads from overloading the filter capacitors of the LCL-filter. Interfacing with higher order filters can also further improve the export of reactive power to the grid or cause even higher attenuation of the voltage ripple caused by the PWM switching frequency. The advantages of using a third order (LCL) filter are investigated explicitly in [57, 58, 59].

The inverter-LCL filter circuit is shown in Fig. 3.9. The state space representation of this system can be written as follows:

$$\frac{dv_c}{dt} = \frac{1}{C}(i_{inv} - i_o) \tag{3.22}$$

$$\frac{di_{inv}}{dt} = \frac{1}{L1}(-v_c + v_{inv} \tag{3.23}$$

$$\frac{di_o}{dt} = \frac{1}{L2}(v_c - v_g) \tag{3.24}$$

In matrix form:

$$\begin{bmatrix} \frac{dv_c}{dt} \\ \frac{di_{inv}}{dt} \\ \frac{di_o}{dt} \end{bmatrix} = \begin{bmatrix} 0 & \frac{1}{C} & \frac{-1}{C} \\ \frac{-1}{L1} & 0 & 0 \\ \frac{1}{L2} & 0 & 0 \end{bmatrix} \begin{bmatrix} v_c \\ i_{inv} \\ i_o \end{bmatrix} + \begin{bmatrix} 0 \\ \frac{1}{L1} \\ 0 \end{bmatrix} v_{inv} - \begin{bmatrix} 0 \\ 0 \\ \frac{1}{L2} \end{bmatrix} v_g \tag{3.25}$$

Thus, the linear time invariant state space equations, for the open loop system, are of the form:

$$\left[\frac{dX(t)}{dt}\right] = [A][X(t)] + [B]v_{inv} - [C]v_g \tag{3.26}$$

where: X(t) : system's state vector $[v_c; i_{inv}; i_o]$;

A, B, and C: constant matrices; the system parameters;

v_{inv}, v_g : Dynamic voltage values at the inverter output and at the point of common connection; respectively.

In the controlled mode, where feedback loop(s) are present, all these parameters can be designed for a specified controller as, [60, 61].

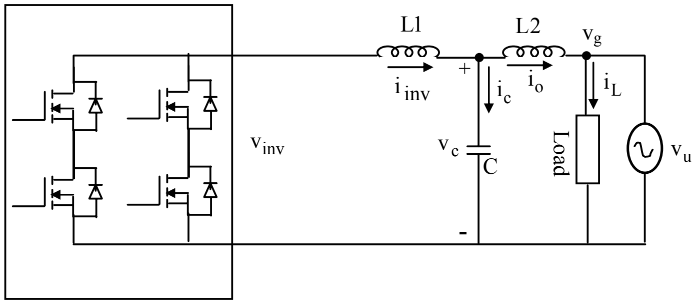

Fig. 3.9: Inverter-LCL filter-grid connection PV system

3.4 Daily load profile model

In order to extract the whole PV generated energy, the inverter controller, using a lookup table, needs knowledge of load profile model. In spite of its random feature, it can be used as guide for a preliminary design.

The load pattern is achieved by listing the power demand of load kinds, number of hours of use per day, and operating voltage. In this work, a proposed optimal pattern of daily operation will perform by taking into the consideration each of: load characteristics, PV generation, and utility demand.

According to possible power flow conditions among the system components, the operation of the proposed system can be cataloged into three main operation modes, as shown in Fig. 3.10. Since each component has its own cost and characteristics for power generation or consumption, an operation of the proposed system is designed with consideration of the following factors, [23, 49]:

1) Load characteristic of the homeowner

From the viewpoint of the homeowner, the best policy is to minimize the kilowatt hour cost from the utility and sell excess power to the utility in its peak- load period demand. For this reason, the load characteristic of the homeowner should be explored;

2) Generation characteristic of the PV power

For a roof-mounted PV array, the insolating level and the solar path are changed with time, and the daily generation characteristic of the PV power should be analyzed for determining the best way to utilize the PV power;

3) Power leveling demand of the utility

A typical power-leveling demand of the utility is to share the peak-load burden of the utility with the off-peak utility power to reshape the power level of the utility.

Based on these considerations, if the daily power profile related to each factor is prescribed, it is possible to determine an optimal pattern of daily operation from the viewpoint of the utility, as well as the homeowner. Fig. 3.11 shows a design example, where the homeowner is atypical modern family, [23].

The daily operation is formed by the operation modes shown in Fig. 3.10 and arranged in sequences as follows, [23]:

- Off-peak load period (Mode1): from midnight to daybreak, the PV power is absent and the load is supplied by the utility;
- Low-insolation period (Mode2): In early morning, the PV power is present, yet not large enough to supply the load power; the insufficient is supplied by the utility;
- High-insolation period (Mode3): from the late morning to middle evening, the PV power is larger than for supplying the load, the excess power can be fed to the utility;
- Low-insolation period again (Mode4 ≡ Mode2): from late evening to sunset ;
- Off-peak load period again (Mode5 ≡ Mode1): from sunset to midnight.

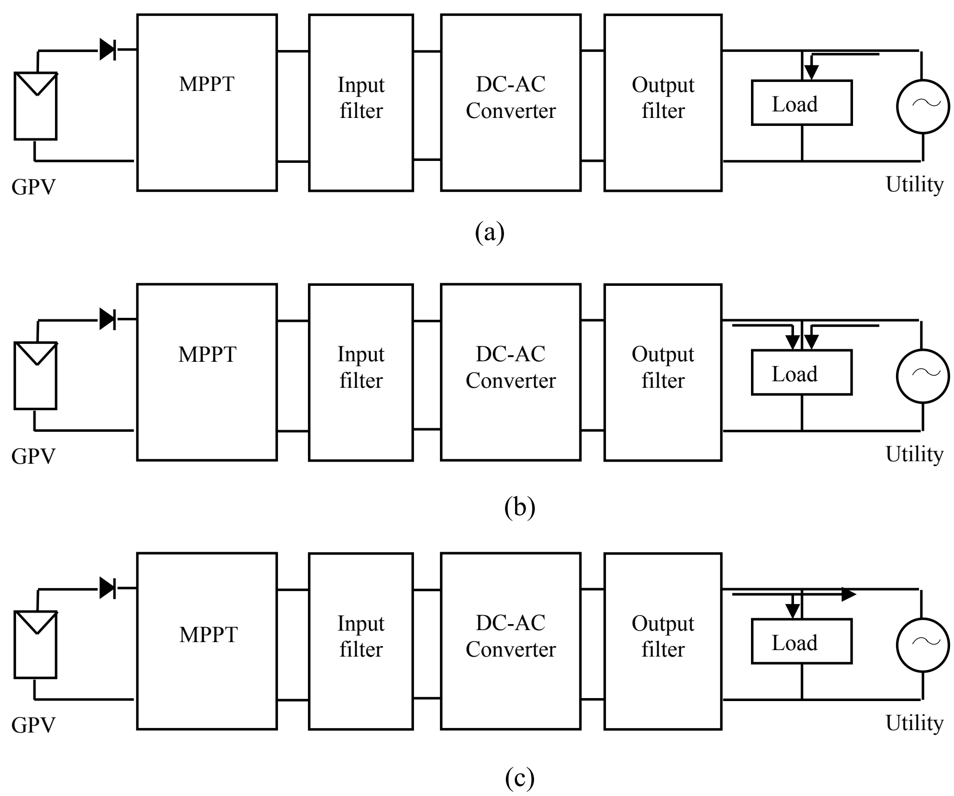

Fig. 3.10: The operating modes of the proposed PV grid-connected system.
(a) Mode1 (b) Mode2 (c) Mode3

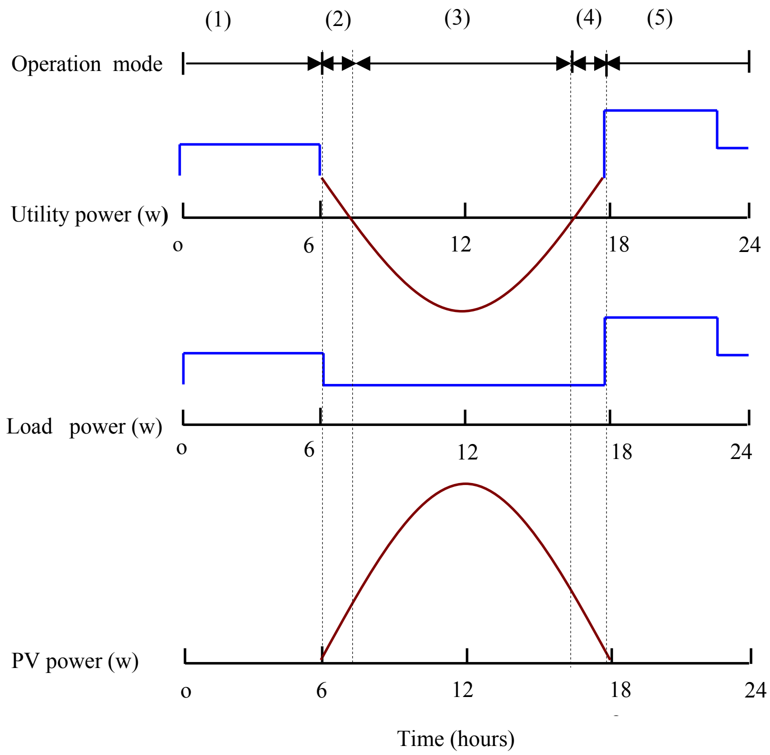

Fig. 3.11: A pattern of daily operation of the proposed load

3.5 Conclusion

In this chapter, firstly a global configuration of the PV grid connected is presented. Then each component of this configuration is modeled by a convenient mathematical or algorithmitical representation. The PV array is described by its I-V characteristics and the inverter with its controllers are briefly described by some examples. While two famous MPPT techniques are illustrated by their algorithms. Finally, a load pattern, for an optimal energy extraction, is proposed in order to predict any optimal control design parameters.

4.1 Introduction

In any system development, two steps are compiled: design and dynamic study. Based on the work achieved, the last step seems to be more justified.

This chapter presents how the components of the proposed system are implemented in Matlab/Simulink environments.

The dynamic behavior of the system will be investigated, using the Matlab/Simulink tools, in order to show the interaction between different parameters of the PV grid connected. According to the main purposes which emphasis on the interaction between parameters, the PowerSim tool and the simplest current controller are used.

4.2 Photovoltaic array simulation

The PV array is composed of 6 parallel branches each branch consists of 18 series modules. The PV module characteristics are given in appendix A.

Simulink gives the user flexibility to build hierarchical models meaning that each block can contain other blocks or other levels, [15]. Fig. 4.1a, shows the blocks that are "hidden" inside the PVG block (Fig. 4.1b). It represents the detailed Simulink implementation of the mathematical model of the PV system as already discussed (equations: (3.5), (3.6), (3.7)). The first output from the PV system block is the array's voltage, and the second output from the block is the array's current. The whole PVG associated to the measurement instrumentations with irradiation and the cell temperature as inputs are shown in Fig. 4.1b.

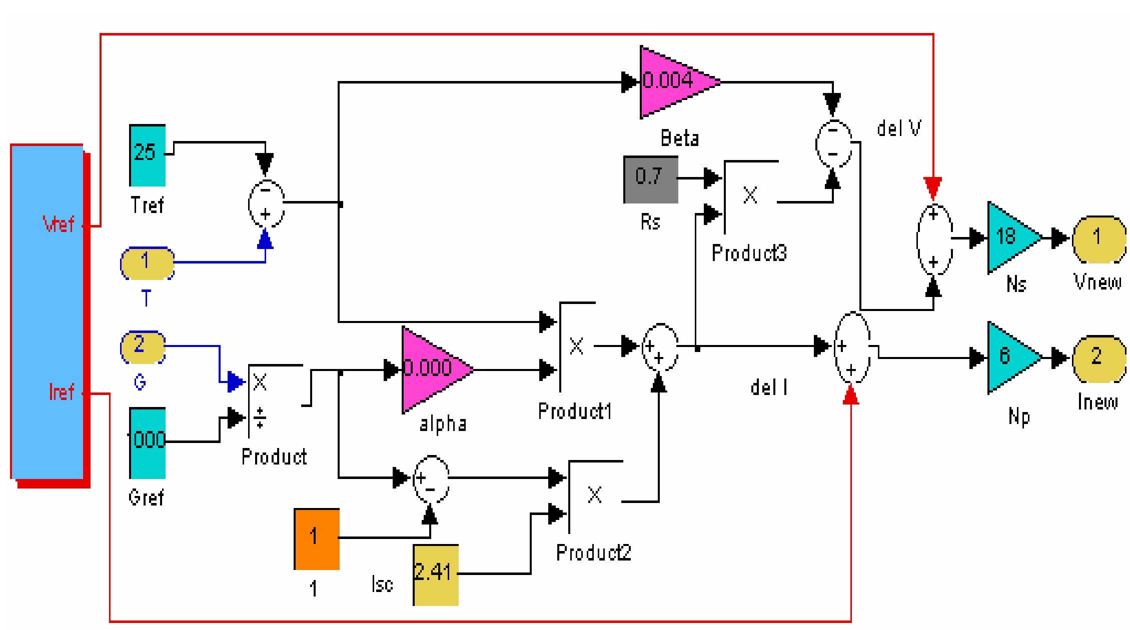

(a)

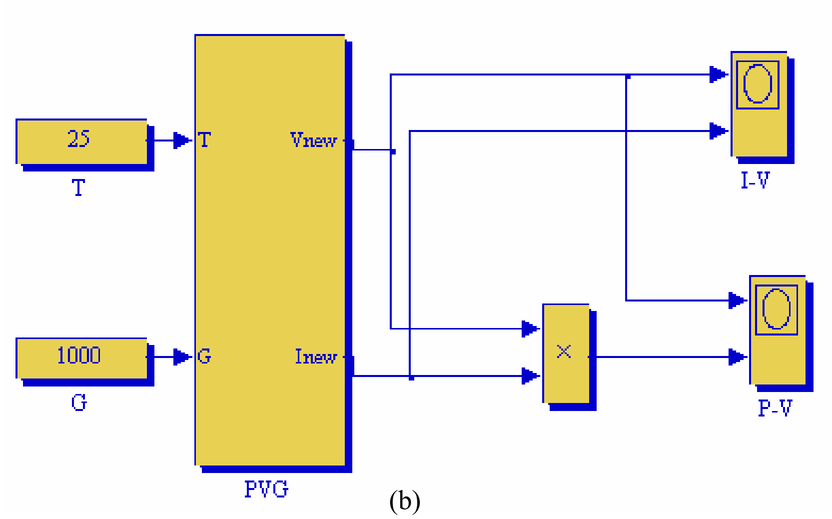

(b)

Fig. 4.1: Simulation of the PV array
(a) Unmasked PVG blocks (b) PVG masked blocks.

In order to show the different zones of the I-V and P-V characteristics, for the purpose of exploiting the maximum power, the I-V and P-V simulations are carried out using the PVG simulink blocks. The results are given in the Fig. 4.2 at standard conditions, where the maximum power is P_{max} =4160W, corresponding to I_{max} =13A and V_{max} = 320V.

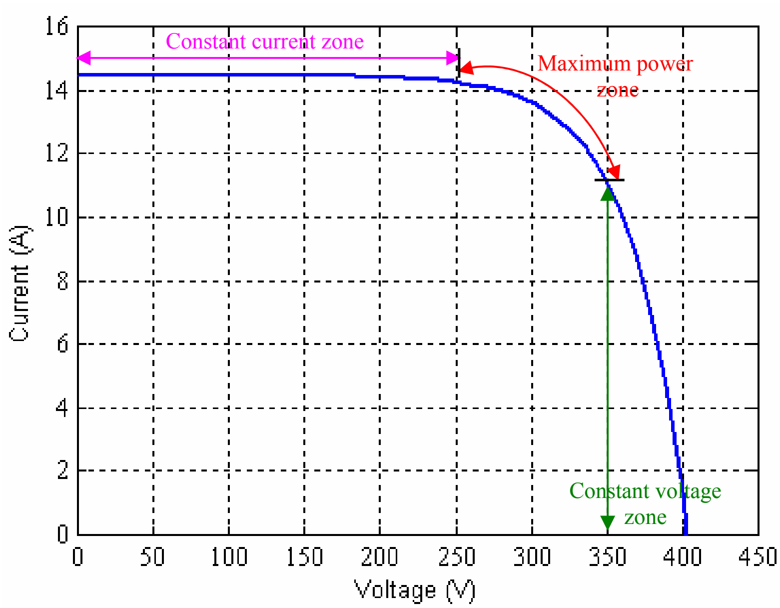

(a)

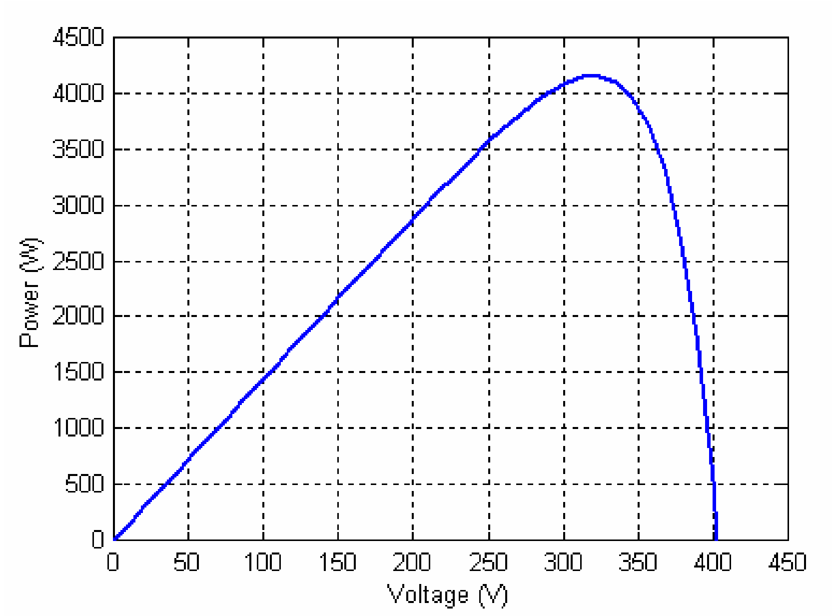

(b)

Fig. 4.2: Simulation results
(a) I-V characteristics (b) P-V characteristics.

The dynamic behavior of the PVG output under the variation of irradiation and temperature, using the modified added model (equations: 3.8-3.14), is analyzed adding these variations as masked blocks or lookup table. The results are given in Fig. 4.3.

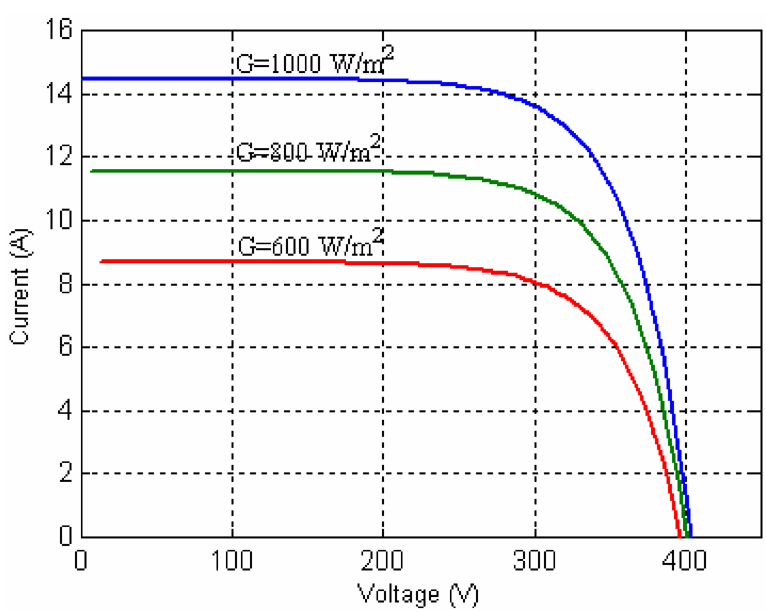

(a)

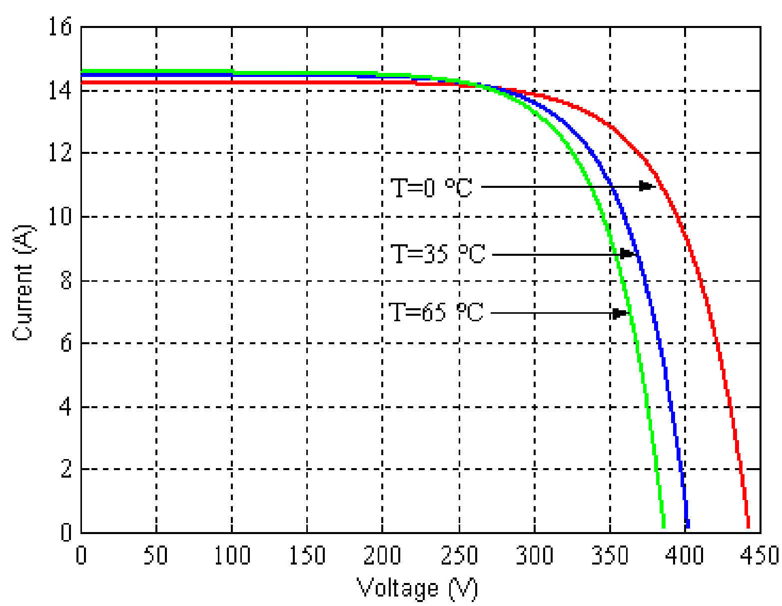

(b)

Fig. 4.3: The effect of temperature and irradiation on I-V characteristics.
(a) Variation of irradiation (b) Variation of temperature

Interpretation of results

Fig. 4.2a illustrates the manner of I-V characteristics which can be divided into two segments or zones separated by the knee of the curve (MPP location). One segment is the constant voltage segment and the other is the constant current segment.

Fig. 4.2b illustrates the P-V characteristics. It shows that there is a linear proportionality, from zero coordinates till the MPP location and then any increasing in the voltage followed by decreasing in the power to reach its zero value at V_{OC}.

Fig. 4.3 shows the effect of temperature and insolation on the I-V characteristics. From Fig. 4.3a, it was observed that the short circuit current of the PV module depends exclusively linearly on the irradiation ($I_{SC} = kG_a$), while the open-circuit voltage V_{OC} increases logarithmically with irradiation. But, Fig. 4.3b shows that increasing cell temperature would decrease the open circuit voltage where it may consider the dominant effect of temperature, because there is only a light increasing of the short circuit current, [15].

4.3 PVG-MPPT simulation

Since it is hard to adjust the operating condition of the PV array, such as the insolating level and temperature in the real field test, many technical methods are proposed in the last chapter. But in this study a script program is developed then is called using S-Function in Simulink environment under the implementation achieved by the block diagram shown in Fig. 4.4.

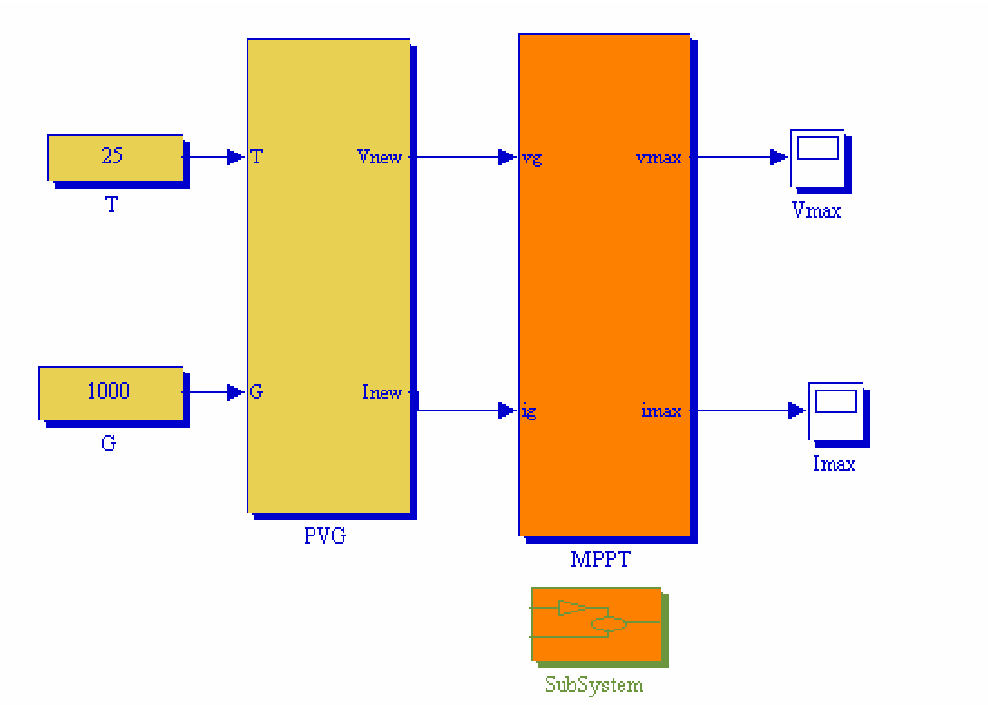

Fig. 4.4: PVG-MPPT block diagram

Simulation result is shown in Fig. 4.5; where the MPPT block trackes the MPP at different insolation levels for example.

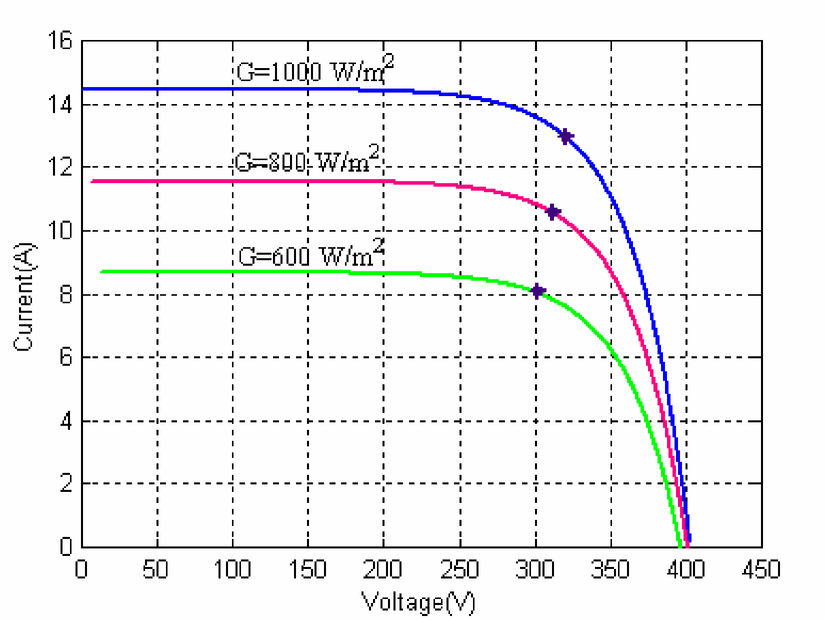

Fig. 4.5: MPP with variation of the insolation levels

Interpretation of results

The MPP is denoted by a cross located at the knee of the I-V curve. The simulation is implemented for different insolation levels where it is observed that for every condition (insolation), each curve has its MPP which is the optimal operating point for the efficient use of the solar array. The coordinates of this point (Vmax and Imax), will be delivered to be interfaced with the grid.

4.4 Simulation of the inverter and its control system.

The simulating block diagram of this system is shown in Fig. 4.6. The inverter and its control technique is investigated without any load, while with the presense of the grid. The power system elements are simulated using PowerSim meanwhile the control part is presented using Simulink components, where both enviroments are interfaced by a suitable elements. The parameter values are given in appendix B.

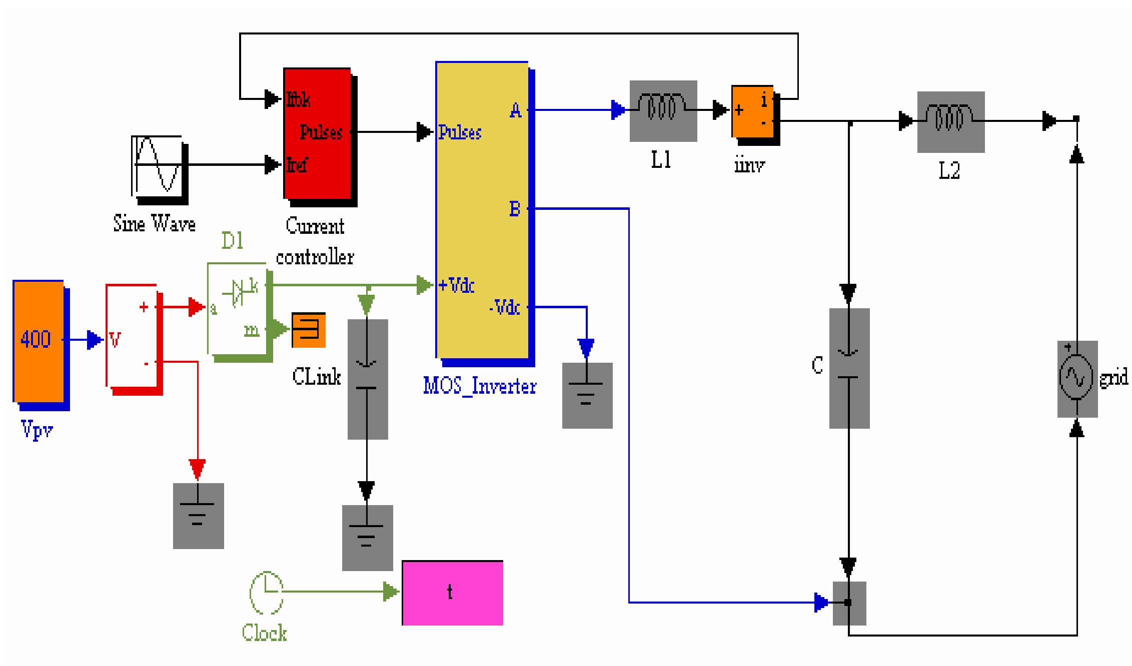

Fig. 4.6: Simulation block diagram of the grid connected PV system and its controller

The simulation results are given in the Figs. 4.7 and 4.8. They show the inverter outpt waveforms: current and voltage (before and after passing the filter).

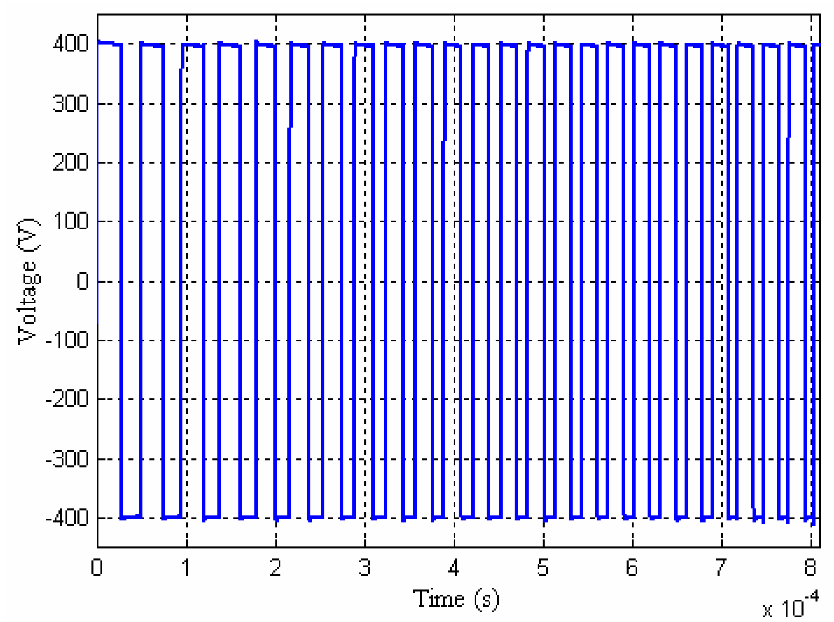
400
300
200
100
0
-100
-200
-300
-400
Voltage (V)
0
1
2
3
4
5
6
7
8
Time (s)
x 10^-4

(a)

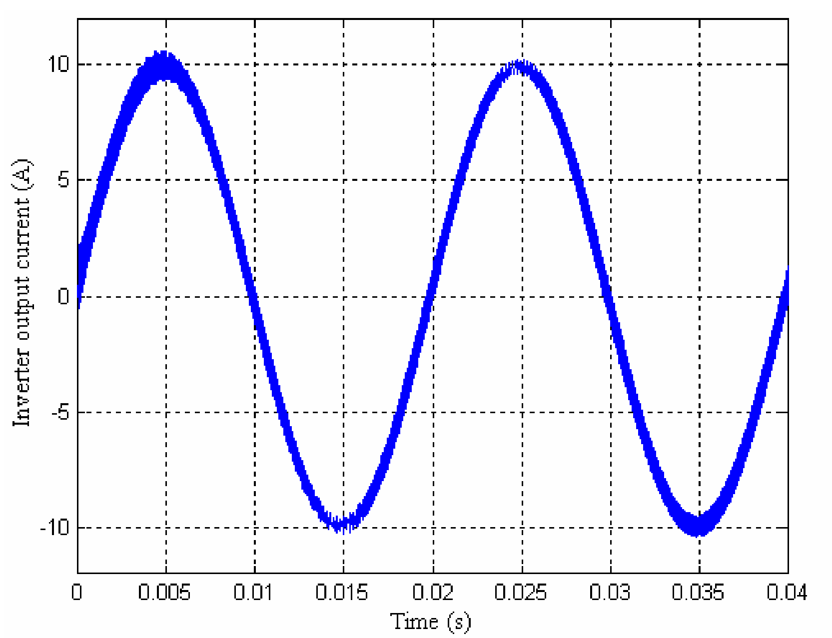
10
5
0
-5
-10
Inverter output current (A)
0
0.005
0.01
0.015
0.02
0.025
0.03
0.035
0.04
Time (s)

(b)

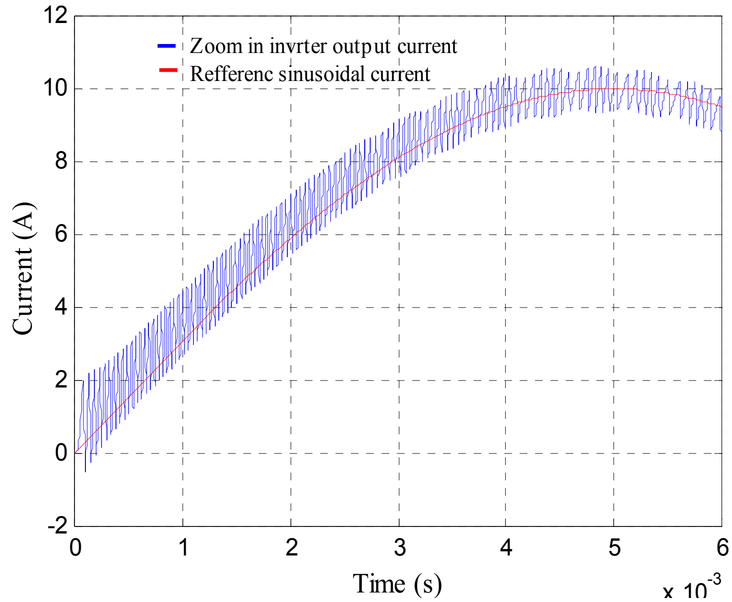

(c)

Fig. 4.7: Inverter outputs.
(a) Output voltage (b) Output Current (c) Zoomed output current

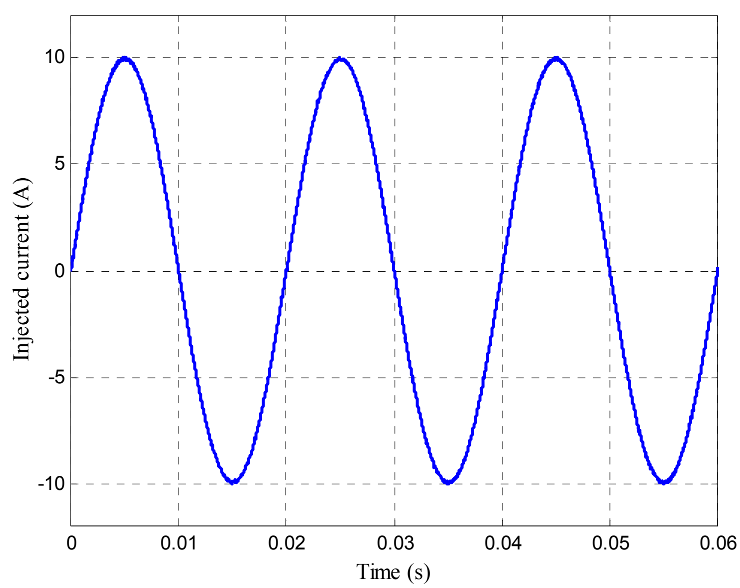

(a)

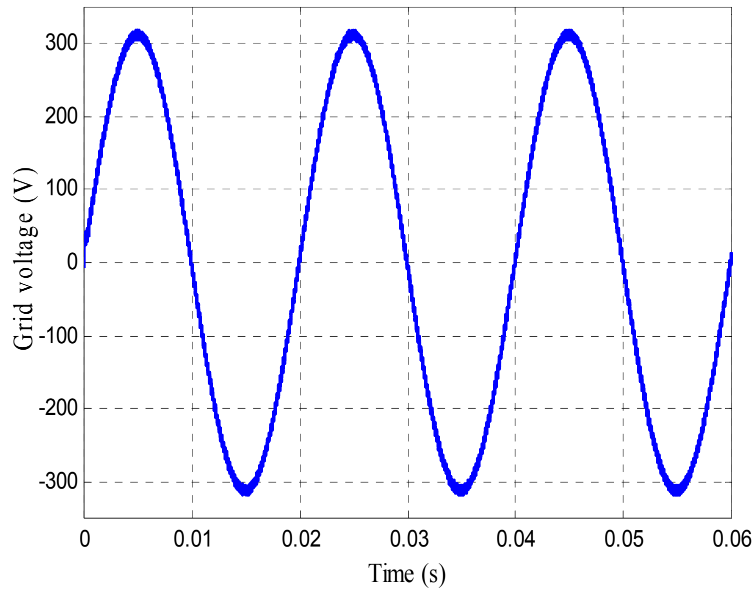

(b)

Fig. 4.8: Filtered inverter outputs.
(a) Voltage waveform (b) Current waveform

Interpratation of results

In the simulation block diagram represented by Fig. 4.6, the MOSFET-inverter is supplied by a DC link voltage (V_{PV}) and loaded by the grid directly, through an LCL filter .

Fig. 4.7 shows the simulation results of the inverter output before passing the filtering system. Fig. 4.7a indicates that the inverter output voltage has a high frequency chopped rectangular waveform (bipolar PWM). In Fig. 4.7b the ripples wides are appeared clealy in the inverter output current, however it follows its reference sinewave as in Fig. 4.7c.

It is clear that, when the inverter output voltage and current passed through a filter, pure sinewaves (220 V/50 Hz, and 7.071 A/50 Hz) are obtained as shown in Figs. 4.8a and 4.8b. These waves can be directly connected to the grid or supplying any AC domestic loads.

This simulation indicates that the filter output current in phase with the utility voltage which is habitually required in such application.

4.5 Simulation of daily operation modes

Fig. 4.9 shows the block diagram simulating the grid-connected PV system, where the overall system is integrated to show the system dynamic behavior. The overall system consists of the previous configuration completed with a PVG, MPPT and a local residential load. In addition to the dynamic behavior, this simulation attempts to show the power flow exchange between different components of the system.

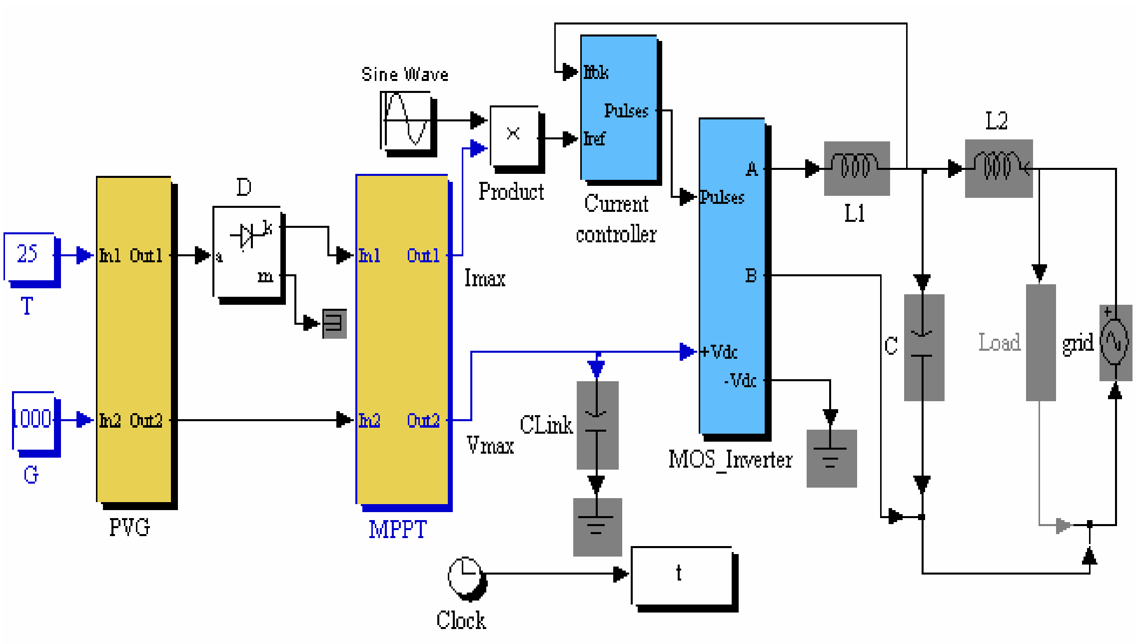

Fig. 4.9: Block diagram of the overall grid-connected PV system

Fig. 4.10 shows the simulation results of the overall system, by taking into account the running conditions of the system in many different periods of time (modes of operation).

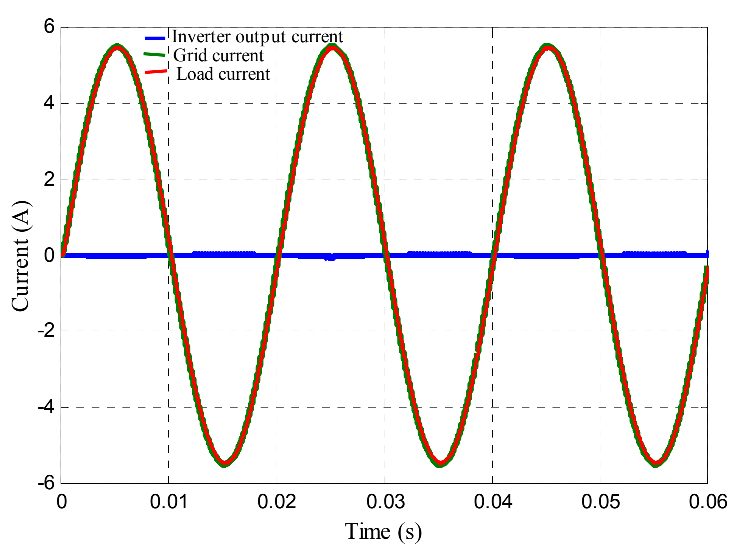

(a)

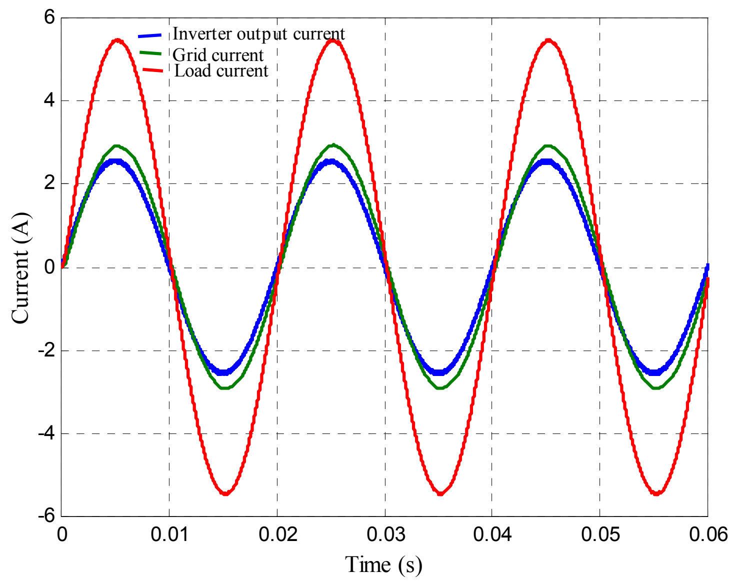

Inverter output current
Grid current
Load current
6
4
2
0
-2
-4
-6
Current (A)
0
0.01
0.02
0.03
0.04
0.05
0.06
Time (s)

(b)

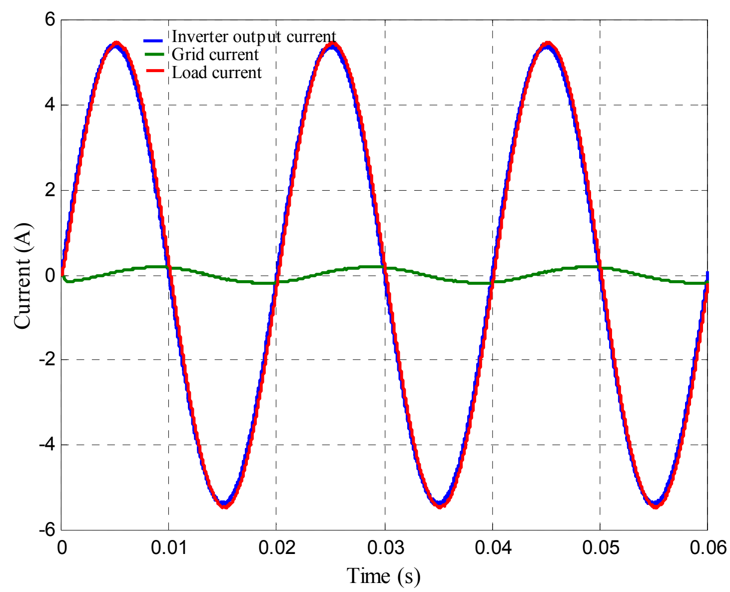

Inverter output current
Grid current
Load current
6
4
2
0
-2
-4
-6
Current (A)
0
0.01
0.02
0.03
0.04
0.05
0.06
Time (s)

(c)

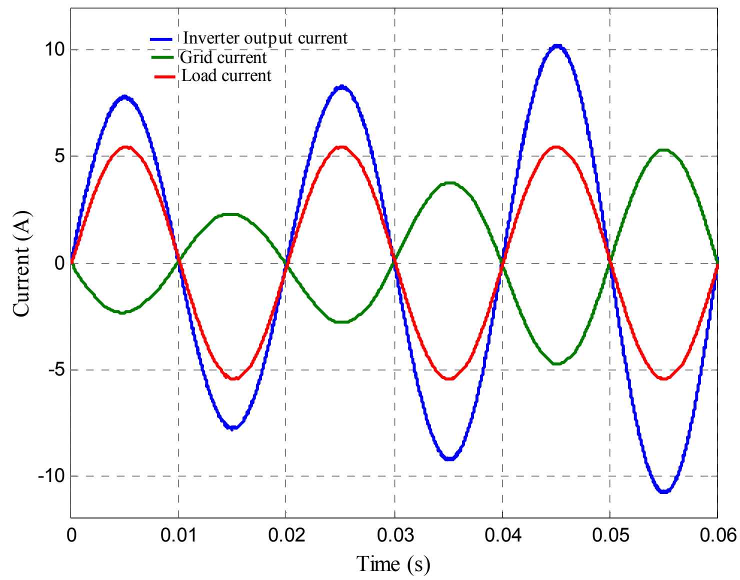

(d)

Fig. 4.10: Operation modes.
(a) Absence of insolation period (b) Low insolation period
(c) Autonomous period (d) High insolation period

Interpretation of results

Based on the consideration of the daily load demand and the weather conditions, this simulation is focused to assume some instants whereas the system is predicted to respect the daily operation modes which were assumed in chapter 3. For achieving that, the irradiation was increased gradually from zero until its maximum value. The suitable results are given in the curves as shown in Fig. 4.10, where:

Fig. 4.10a shows that, the PV energy is zero and the load is completely supplied by the utility. This condition usually happens at nighttimes or at short specific weather conditions where the PV array may be covered quietly by a cloud.

Fig. 4.10b indicates that there is insufficient PV energy whereby the utility is concerned to cover this shortcoming of energy. This condition usually occurs at low insolation periods, in early morning or late evening.

Fig. 4.10c shows an auto-sufficient period where the PV energy is just able to supply the load. Like these conditions characterize by its short duration.

Fig. 4.10d illustrates that the PV energy is large than load demands; the excess energy is will be exported to the utility. The suitable times for that are usually from late morning to middle evening.

All modes of operation are integrated together in the appendix C.

4.6 Conclusion

In this chapter, the proposed system components are implemented in Matlab/Simulink environments. The dynamic behavior of the system is investigated, using the Matlab/Simulink tools, showing the interaction between different parameters of the PV grid connected.

In addition to the dynamic behavior investigation, the simulation has showed the power flow exchange between different components of the system for different modes of operation.

General conclusion

The objective of this work is to contribute in studying of the grid-connected photovoltaic (PV) system supplying a residential load. An overall view of the PV system was developed, followed by the presentation of different structures of the grid-connected PV systems.

For the purpose of designing and implementing such systems, the mathematical model for each chain's element was found. These models have permitted to show the dynamic behavior of the system at the connected point; by taking into account that the PV generator operates at its maximum power point (MPP).

The obtained models were simulated with their operation modes as a grid-connected system. Simulations showed that the PV system output power varies with irradiation and cell temperature. A good dynamical comportment of the system have been observed, for different climatic conditions (irradiation and temperature) as well as for a given load profile. This is due to the selected control strategy named adaptive or hysteresis technique.

In the future, it is suggested to look for the following:

- Studying the different control strategies of the grid-connected PV systems using the set of models presented in this work with or without the presence a set of battery bank;
- Development of an experimental prototype of a grid-connected PV system for a specified application (residential in two different weather zones: hot and cold).

Appendix A:

Table 1: PV module characteristics at: T_{ref}=25°C, G_a=1000 W/m^2

Parameter	***Value***
Short circuit current	2.41 A
Open circuit voltage	22.4 V
Maximum voltage	17.45 V
Maximum current	2.2 A
Series resistance	0.7 Ω
Current temperature coefficient	α =0.6 %/°C
Voltage temperature coefficient	β =4 %/°C
Module section	0.4 m^2

Appendix B:

Table 1: Power circuit parameters

Element	***Value***
Inverter input filter	C_{Link}=300 µF
Inverter output filter	L1= 5 mH L2=5 mH C= 3 µF
Utility grid	220V/50 Hz

Appendix C:

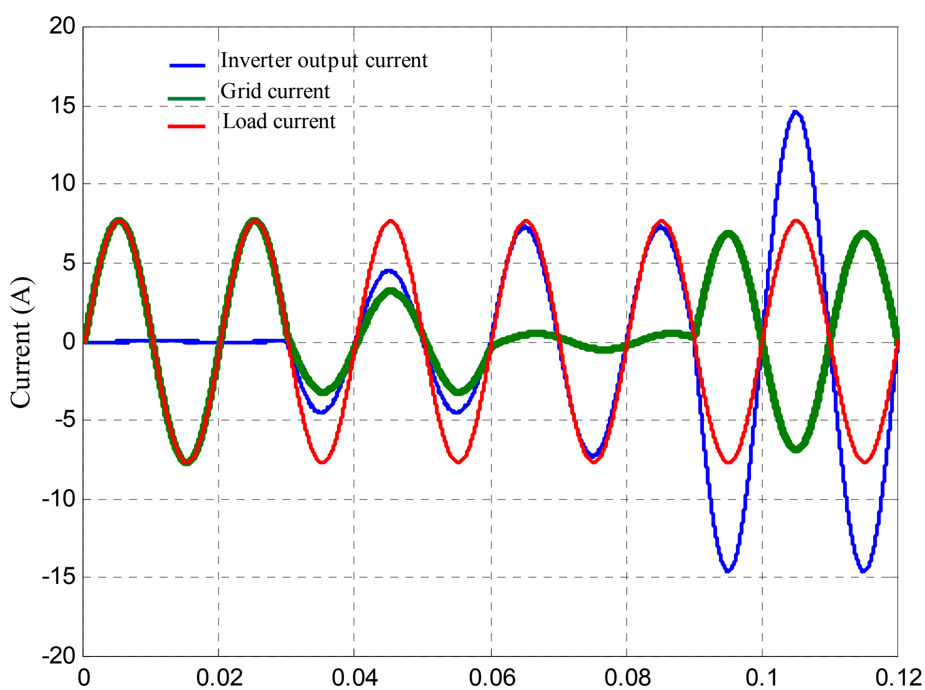

Fig. 1: Modes of operation of the system

References

[1] I. M. Ballard, "Electrical and optical characterization of MQW solar cells under elevated temperatures and illumination levels", PhD, Physics Department, University of London, October 1999.

[2] F. Kininger, "Photovoltaic Systems Technology", Master thesis, Universität Kassel, Germany, 2003.

[3] H. Hadi, "Photovoltaic water pump system", PhD, Kochi University of Technology, August 2003.

[4] T. F. Wu, C. H. Chang, Y. K. Chen, "A multi-function photovoltaic power supply system with grid-connection and power factor correction features", IEEE 31stAnnual conference on power electronics specialists PESC'2000, Vol. 3, PP. 1185-1190, 2000.

[5] L. G. Leslie, "Design and analysis of a grid-connected photovoltaic generation system with active filtering function", Master thesis, Virginia Polytechnic Institute and State University, March 2003.

[6] P. Ludovic, A. Stéphan, "Convertisseurs photovoltaïc", Technique de l'ingènieur, 1997.

[7] B. Maria, "Optical efficiency of low-concentrating solar energy systems with parabolic reflectors", PhD, Uppsala university, Sweden, 2004.

[8] J. W. Twidell, A. D. Weir, "Renewable energy resources", University press, Cambridge, Great Britain, 1986.

[9] W. Achim, "Design issues of photovoltaic systems and their grid integration", PhD, U. K. Leuven, December 2003.

[10] T. Markvart, "Photovoltaic solar energy conversion", Summer University: Energy for Europe, 2002. http://www.physique-u-strasbg.fr/uee

[11] M. Djarallah, B. Azui, "Optimisation model for grid-connected interactive photovoltaic system", First Baha technical meeting BTM'2004, Kingdom of Saudi Arabia, May 2004.

[12] A. Btka, "Optimisation d'un system de pompage photovoltaic au fil du soleil", Magister en électrotechnique, Institut d'électrotechnique, Centre Universitaire Mohamed Khider Biskra, 1997.

[13] M. Capderou, "Atlas solaire de l'Algérie. T3 Aspect géométrique, synthèse géographique", Office des publications Universitaires, Vol. 2, Alger, Algérie, 1986.

[14] C. Hamouda, "Theoretische und experimentelle Untersuchungen von photovoltaischen Pumpsystemen im Aurès-Gebirge in Algerien", Dissertation Universität Berlin, 1997.

[15] D. Hancen, H. Lars, H. Bindner, "Models for stand-alone PV system", Riso National Laboratory, Roskilde, Norway, December 2000.

[16] N. W. Joseph, "An interactive menu-driven design tool for stand-alone photovoltaic system", Master thesis, Faculty of the Virginia Polytechnic Institute and State University, January 1998.

[17] A. labouret, M. Villoz, "Energie solaire photovoltaïc", Edition Dunod, Paris, 2003.

[18] O. Gergaud, B. Multon, H. Ben Ahmed, "Analysis and experimental validation of various photovoltaic system models", 7th International ELECTRIMACS Congress, Montréal, August 2002.

[19] H. Chihchiang, S. Chihming, "Study of maximum power tracking techniques and control of DC/DC converters for photovoltaic power system", IEEE 29th Annual conference on power electronics specialists PESC'98, Vol.1, PP. 86-93, May 1998.

[20] W. Geoff, "Evaliating MPPT converter topologies using a Matlab PV model", Journal of electrical & electronics engineering, Vol. 21, N^0 1, Australia, 2001.

[21] B. Carlos, B. Domingo, M. Juan, G. Francesc, "Boost-buck inverter variable structure control for grid-connected photovoltaic systems", IEEE Proceedings of the international symposium on industrial electronic ISIE'2005, Vol. 2, PP. 657-662, June 2005.

[22] M. Faizal, "Grid-connected photovoltaic system", Master thesis, University of Queensland, May 2003.

[23] S. J. Chiang, K. T. Chang, C. Y. Yen, "Residential photovoltaic energy storage system", IEEE Transactions on industrial electronics, Vol. 45, PP. 385-394, June 1998.

[24] F. Labrique, "Les convertisseur de l'électronique de puissance: Tome 5: Command et comprtement dynamique", Technique et documentation, La voisien, 1998.

[25] G. Seuir, F. Labrique, "Les convertisseur de l'électronique de puissance: Tome 4: La conversion continu-alternatif", Technique et documentation, La voisien, 1995.

[26] T. J. Starrs, "Barriers and solutions to interconnection issues for solar photovoltaic systems", Conference proceedings of the first world conference on photovoltaic energy conversion, Vol. 3, PP. 793-806, December 1994.

[27] S. J.Huang, F. S. Pai, "Design and operation of grid-connected photovoltaic system with power-factor control and active islanding detection", IEE Proc.-Gener. Transm. Dirtrib., Vol. 148, N^o 2, March 2001.

[28] R. J. Hacker, "Electricity generation by commercial customers using photovoltaic grid-connection", IEEE Colloquium on electricity generation by commercial customers using photovoltaic (digest N^0 1994/199), October 1994.

[29] S. Kiyoshi, "National survey report of PV power applications in Japan 2002", IEA International Energy Agency, May 2003.

[30] "Australia – National Status Report", http:/www.euronet.n1/users/oke/PVPS/nsr/aus.htm (current 11th of May 2003).

[31] M. Dai, M. N. Marwali, J.W. Jung, and A. Keyhani, "Power flow control of a single distributed", IEEE Power systems conference and exposition, Vol. 1, pp. 398-403, October 2004.

[32] F.L. Albuquerque, A. J. Moraes, G. C. Guimarks, S. M. R. Sanhueza, A. R. Vaz, "Optimization of a photovoltaic system connected to electric power grid", IEEE Transmission and distribution conference and exposition, PP. 645-650, Latin America, 2004.

[33] T. Brekken, C. H. Lana, R. Moumneh, "Utility-connected power converter for maximizing power transfer from a photovoltaic source while drawing ripple-free current", IEEE 33rd annual power electronics specialists conference, Vol. 3, PP. 1518-1522, June 2002.

[34] Y. C. Kuo, T. J. Liang, J. F. Chen, "Novel maximum power point tracking controller for photovoltaic energy conversion system", IEEE Transaction on industrial electronics,

Vol. 48, PP. 594-601, June 2001.

[35] M. Calais, J. Myrzik, T. Agelids, "Inverters for single-phase grid connected photovoltaic system-an overview", IEEE 33rd Annual power electronics specialists conference, vol. 4, PP. 1995-2000, June 2002.

[36] J. M. Myrzik, M. Calais, "String and module integrated inverters for single-phase grid connected photovoltaic systems - A review", IEEE Power technology conference proceedings, Vol. 2, PP. 8, June 2003.

[37] B. Azoui, "Concept and realization of a three phase brushless dc motor for solar applications", PhD thesis, Batna University, 2002.

[38] H. Chihchiang, L. Jongrong, S. Chihming, "Implementation of a DSP-controlled photovoltaic systemwith peak power tracking", IEEE Transactions on industrial electronics, Vol. 45, PP. 99-107, February 1998.

[39] C. T. Pan, T. Y. Chang, "An improved hysteresis current controller for reducing switching frequency", IEEE Transactions on power electronics, Vol. 9, N^0 1, January 1994.

[40] F. Zerhouni, M. Zegrar, "Approche dans la modelisationd'un generateur photovoltaïque", International conference on electronics ICEL'2000, PP. 364-368 Oran, Algeria, November 2000.

[41] C. T. Pan, J. C. Chen, Y. S. Huang, "A fast maximum power point tracker for photovoltaic power systems", IEEE Annual conference of industrial electronics society IECO'99, Vol. 1, PP. 390-393, December 1999.

[42] V. Quaschning, R. Hanitsch, "Numerical simulation of photovoltaic generators with shaded cells", 30th Universities power engineering conference, PP. 583-586, Greenwich, September 1995.

[43] D. M. Baker, G. **V.** Nayar, "A comparison of tri-level and bi-level current controlled grid-connected single-phase full-bridge inverters", IEEE Proceedings of the international symposium on industrials ISIE'97, Vol. 2, PP. 663-668, July 1997.

[44] D. M. Baker, V. G. Agelidis, C. V. Nayar, "Simulation of full-bridge current-controlled grid-connected inverter system", www.at.net.au/index.aspx

[45] B. K. Bose, "Power electronics and drives", Prentice-Hall, 1986.

[46] M. H. Rashid, "Power electronics, circuits, devices, and applications", Prentice-Hall, Inc., 1988.

[47] A. M. Trzynadlowski, "Introduction to modern power electronics", John Willey & Sons, Inc. 1998.

[48] K. M. Rahman, M. R. Khan, M. A. Choudhury, M. A. Rahman, "Variable-band hysteresis current controllers", IEEE Transactions on power electronics, Vol. 12, N^0 6, November 1997.

[49] E. Endo, K. Kurokawa, "Sizing procedure for photovoltaic systems", IEEE First WCPEC, Hawaii, December 1994.

[50] Y. Jung, G. Yu, J. Choi, "High frequency DC link inverter for grid-connected photovoltaic system", IEEE Photovoltaic specialists conference, Vol. 2, PP. 1410-1413, May 2002.

[51] M.N. Marwali, A. Keyhani, "Control of distributed generation systems, Part I: voltages and currents control," IEEE Transactions on power electronics, Vol. 19, PP. 1541-1550, November 2004.

[52] E. J. Davison, B. Scherzinger, "Perfect control of the robust servomechanism problem," IEEE Transictions on automatic Control, vol. 32, PP. 689-702, August 1987.

[53] H. Dehbonei, C. Nayar, L. Borle, "A combined voltage controlled and current controlled 'Dual Converter' for a weak grid connected photovoltaic system with battery energy storage", IEEE 33rd Annual power electronics specialists, Vol. 3, PP. 1495-1500, June 2002.

[54] F. Scapino, F. Spertino, "Load curves at DC side: a useful tool to predict behavior and the design to grid-connected photovoltaic systems", IEEE International symposium on industrial electronics, Vol. 3, PP. 981-986, May 2002.

[55] K. Masoud, G. Ledwich, "Sampling averaging for inverter control", IEEE 33rd Annual power electronics specialists conference PESC'02, Vol. 4, PP. 1699-1704, June 2002.

[56] T. Kawabata, T. Miyashita, Y. Yamamoto, "Dead beat control of three phase PWM Inverter", IEEE Transactions on power electronics, Vol. 5, No. 1, PP. 21-28, January 1990.

[57] G. Ledwich, H. Sharma, "Reactive support from photovoltaic inverters", IPEC Conference, PP. 52-57, Singapore, May 1997.

[58] G. Ledwich, "Simple grid interfaces for photovoltaic", IEEE Proceedings of international conference PEDES'98, Vol. 1, PP. 470-474, December 1998.

[59] M. Liserre, F. Blaabjerg, S. Hansen, "Design and control of an LCL-filter-based three phase active rectifier", IEEE Transactions on industry applications, Vol. 41, N° 5, PP. 1281-1291, September 2005.

[60] M. Pinard, "Command d'électronique des moteurs électriques", Edition Dunod, Paris, 2004.

[61] N. A. Rahim, J. E. Quaicoe, "A single phase voltage source utility interface system for weak AC network applications", IEEE Ninth annual conference proceedings on applied power electronics APEC'94, PP. 93-99, 1994.

Abstract

Categorized as one of the renewable energies, Photovoltaic system has a great potential compared to its counterparts of renewable energies. Photovoltaic makes use of the most abundant energy on earth that is sunlight. Distributed generation units with small energy sources, such as the photovoltaic devices, can be connected to utility grid as alternative energy sources besides providing power to their local loads.

In this work, a contribution to the study of the grid connected photovoltaic system is done, taking case of the domestic load as a local load drawing the energy either from the photovoltaic source or from the utility/grid. The overall backgrounds required to design a photovoltaic system together with the conception of the controlled grid connected photovoltaic system are demonstrated. At modeling of the system, different strategies of control are discussed and the hysteresis band current controller is chosen. This scheme employs a single phase voltage source full bridge pulse width modulation inverter and a third order T-filter. The inverter output current is selected to employ a feedback current control in order to ensure sinusoidal load/grid voltage and current in the power circuit.

The dynamic behavior of the system is investigated, using the Matlab/Simulink tools, in order to show the interaction between different parameters of the photovoltaic grid connected system. It shows that the photovoltaic generator is delivered the maximum power to the system. Moreover, the operation modes show that the proposed control scheme offers improve performance for utility interface applications. It is simple to implement and capable of producing perfect sinusoidal current and voltage waveforms.